CAL LAB

THE INTERNATIONAL JOURNAL OF METROLOGY

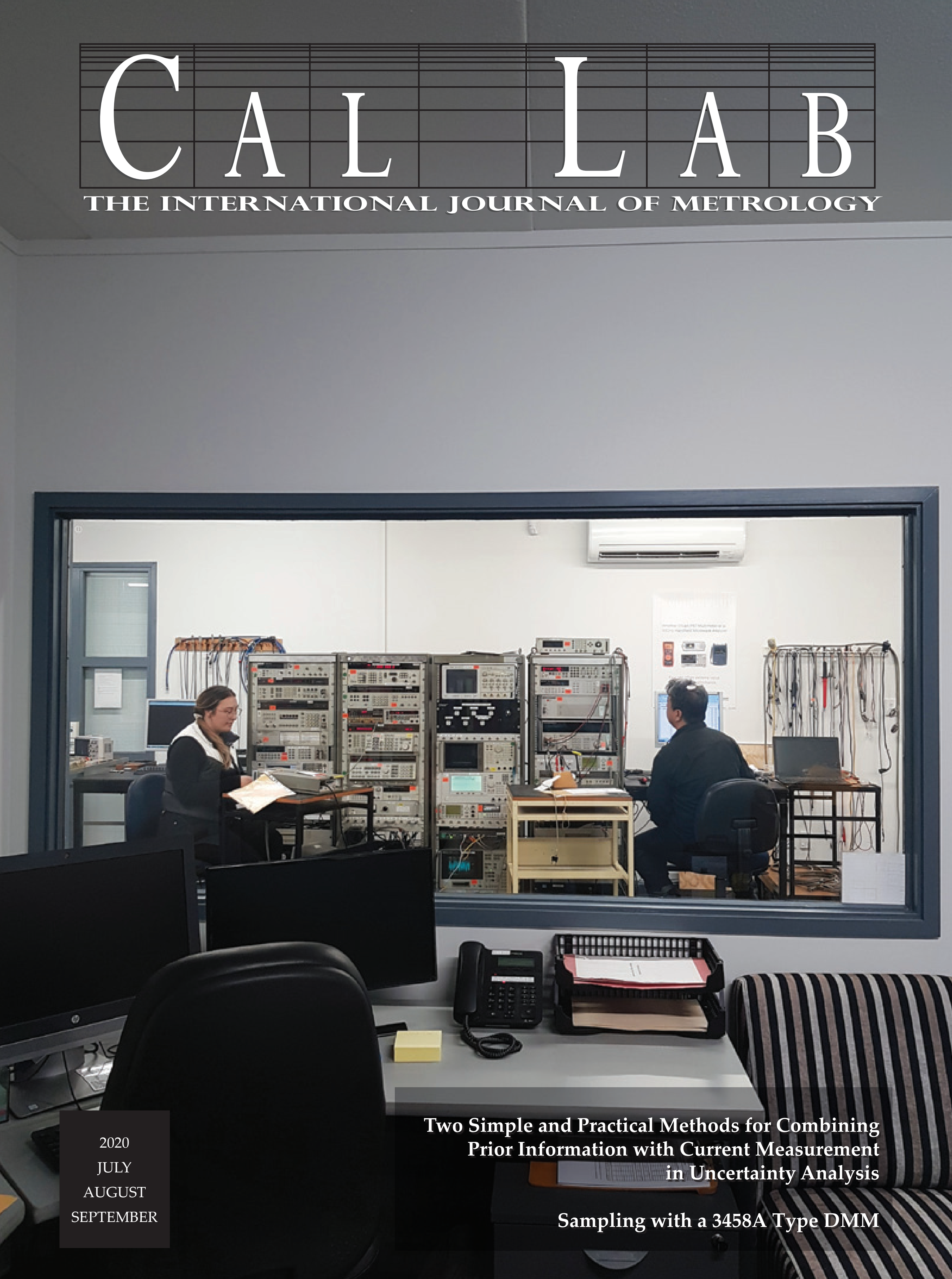

2020
JULY
AUGUST
SEPTEMBER

Two Simple and Practical Methods for Combining Prior Information with Current Measurement in Uncertainty Analysis

Sampling with a 3458A Type DMM

PRECISION CURRENT INSTRUMENTATION AND CURRENT CALIBRATION

DANISENSE HIGH PRECISION CURRENT TRANSDUCERS

± 50A to ± 10000A DC/AC precision fluxgate current transducers for power measurement, battery test systems, high-stability power supplies, and current calibrations.

- Current Ranges 50A ... > 10000A
- Linearity Error down to 2 ppm
- Very high absolute amplitude and phase accuracy from dc to over 1kHz
- Low signal output noise
- Low fluxgate switching noise on the pimary

HIGH CURRENT CALIBRATION SERVICES

Your ability to deliver accurate and reliable measurements depends on the stability of your equipment, and your equipment depends on the accuracy and quality of its calibration.

With over 25 years of calibration experience, GMW offers AC and DC NIST Traceable and/or **ISO/IEC 17025:2005 Accredited*** current calibration services for Current Transducers at our San Carlos, CA location and On-Site for minimal disruption of daily operations.

Transducers manufacturers calibrated by GMW include, but not limited to, Danisense, LEM, GE, ABB, Danfysik, Hitec, AEMC, VAC, PEM, Yokogawa.

** See gmw.com/current-calibration for Scope of Accreditation*

CAL LAB
THE INTERNATIONAL JOURNAL OF METROLOGY
www.callabmag.com

Volume 27, Number 3

FEATURES

DEPARTMENTS

ON THE COVER: RF Test Solutions Ltd delivers ISO 17025 accredited calibration at 41° South (Wellington, New Zealand).

UPCOMING CONFERENCES & MEETINGS

The following event dates are subject to change. Visit the event URL provided for the latest information.

Jan 8-10, 2021 IEEE CMI – Virtual Event. Kolkata, India. The IEEE 2nd International Conference on Control, Measurement and Instrumentation will provide a global forum for academicians, researchers, industrial practitioners, scientists and engineers to discuss about their research endeavors, studies, findings, new ideas and concepts, contributions and developments related to the areas of control theories and applications, measurement theories and applications and instrumentation theories and applications. https://ewh.ieee.org/r10/calcutta/css_ims/CMI2021/index.html

May 3-6, 2021 SMSI. Nuremberg, Germany. Held in conjunction with SENSOR+TEST, Sensor and Measurement Science International will be a hybrid face-to-face and virtual event. The SMSI brings scientists and researchers from all concerned scientific fields together to secure the success of these ideas in the future. https://www.smsi-conference.com/

May 4-6, 2021 SENSOR+TEST. Nuremberg, Germany. Since the SENSOR+TEST trade fair was not allowed to take place in 2020, we have started planning for the next event. From 4 to 6 May 2021 experts will be meeting again for an in-depth exchange on the worldwide most important industrial fair for sensor and measuring technology. www.sensor-test.com

May 17-21, 2021 IEEE I2MTC. Glasgow, Scotland. The IEEE I2MTC – International Instrumentation and Measurement Technology Conference – is the flagship conference of the IEEE Instrumentation and Measurement Society and is dedicated to advances in measurement methodologies, measurement systems, instrumentation and sensors in all areas of science and technology. These features make I2MTC a unique event and one of the most important conferences in the field of instrumentation and measurement. https://i2mtc2020.ieee-ims.org/

Jun 6-11, 2021 IMS. Atlanta, GA. Join us at the intersection of communications, aerospace, automotive, IoT and other emerging technologies to learn the latest developments in MHz-to-THz theory, techniques, devices, systems and applications at the International Microwave Symposium (IMS). IMS2021 is the centerpiece of Microwave Week 2021 comprised of three conferences including the RFIC Symposium (www.rfic-ieee.org) and the ARFTG Conference (www.arftg.org). https://ims-ieee.org/ims2021

CAL LAB
THE INTERNATIONAL JOURNAL OF METROLOGY

PUBLISHER
MICHAEL L. SCHWARTZ

EDITOR
SITA P. SCHWARTZ

CAL LAB
PO Box 111113
Aurora, CO 80042
TEL 303-317-6670 • FAX 303-317-5295
office@callabmag.com
www.callabmag.com

Subscription fees for 1 year (4 issues)
$50 for USA, $55 Mexico/Canada,
$65 all other countries.
Visit **www.callabmag.com**
to subscribe.

Printed in the USA.

ISSN No. 1095-4791

EDITOR'S DESK

Community Revisited

During a recent interview, I touched upon the concept of the metrology community and its importance. It felt right at the time; it made sense as an idealist. But I have scrambled eggs for brains and started to vaguely remember an Editor's Desk I wrote called "Community." So, I dug it out from a couple years ago and it's a bit dark and unfair.

Since then, I've gotten to talk with more people in the industry. With the overwhelming push and pull of work and obligations, a bigger picture comes into view. Now, the distraction is how to fit all the big floating puzzle pieces together. Yes, they are fractured, but how can we make people and ideas work together?

Community can be defined as a group of people living under the same set of laws or an ecological community of plants and animals in a pond. But I think the most appropriate definition for community for metrology is "joint ownership." Through joint ownership, we are not only responsible for verifying the work we do, but also mutual owners of the outcome of our work. Community isn't just networking; it's a lot of hard work and cooperation.

The business end of metrology can be brutal, but it's the fruits of labor at the end of the day, whether it's getting a new issue laid out, passing a lab audit, or organizing an online event, it all requires cooperation among a group of measurement folks. From the magazine end, the measurement community is a lifeline. We depend on our network of professional associates we meet through industry organizations, customers, and by just reaching out!

Hening Huang has been a terrific contributor over the years, with his latest article exploring "Two Simple and Practical Methods for Combining Prior Information with Current Measurement in Uncertainty Analysis." And, Rado Lapuh shares with us his long experience working with the popular 3458A digital multimeter in "Sampling with a 3458A Type DMM."

We encourage metrology professionals in their field to submit their ideas to a wider audience by submitting articles on work they've done, whether diving deep into methodological observations or discovering solutions to complex (or common) issues! We are proud to be part of this measurement community and hope our readers feel the same.

Happy Measuring,

Sita Schwartz
Editor

SEMINARS & WEBINARS: Dimensional

Nov 10-11, 2020 Gage Calibration & Repair. Akron, OH. IICT Enterprises. This 2-day training offers specialized training in calibration and repair for the individual who has some knowledge of basic Metrology. Approximately 75% of the workshop involves "Hands-on" calibration, repair and adjustments of micrometers, calipers, indicators height gages, etc. http://www.calibrationtraining.com/

Nov 17, 2020 Dimensional Measurement User. Bristol, UK. INSHERE Ltd. In this training course, learners will be introduced to dimensional metrology and the importance of good measurement practice and the right measurement behaviors. This is an EAL approved qualification. https://training.npl.co.uk/course/dimensional-measurement-user/

Nov 17-18, 2020 Gage Calibration & Repair. Altoona, WI. IICT Enterprises. This 2-day training offers specialized training in calibration and repair for the individual who has some knowledge of basic Metrology. Approximately 75% of the workshop involves "Hands-on" calibration, repair and adjustments of micrometers, calipers, indicators height gages, etc. http://www.calibrationtraining.com/

Dec 1-2, 2020 Gage Calibration & Repair. Des Moines, IA. IICT Enterprises. This 2-day training offers specialized training in calibration and repair for the individual who has some knowledge of basic Metrology. Approximately 75% of the workshop involves "Hands-on" calibration, repair and adjustments of micrometers, calipers, indicators height gages, etc. http://www.calibrationtraining.com/

Dec 2-4, 2020. Seminar 114: Gage Calibration. Mitutoyo Institute of Metrology. Aurora (Chicago), IL. Mitutoyo America's Gage Calibration course is a unique, active, educational experience designed specifically for those who plan and perform calibrations of dimensional measuring tools, gages, and instruments. https://www.mitutoyo.com/events/categories/educational-seminars/

Dec 9-10, 2020 Gage Calibration & Repair. Bloomington, MN. IICT Enterprises. This 2-day training offers specialized training in calibration and repair for the individual who has some knowledge of basic Metrology. Approximately 75% of the workshop involves "Hands-on" calibration, repair and adjustments of micrometers, calipers, indicators height gages, etc. http://www.calibrationtraining.com/

Mar 2, 2021 Dimensional Measurement User. Bristol, UK. INSPHERE Ltd. In this training course, learners will be introduced to dimensional metrology and the importance of good measurement practice and the right measurement behaviors.

This is an EAL approved qualification. https://training.npl.co.uk/course/dimensional-measurement-user/

May 26-27, 2021 Dimensional Measurement. Port Melbourne, VIC. Australia NMI. This two-day course (9 am to 5 pm) presents a comprehensive overview of the fundamental principles in dimensional metrology and geometric dimensioning and tolerancing. https://shop.measurement.gov.au/collections/physical-metrology-training

SEMINARS & WEBINARS: Electrical

Nov 24-25, 2020 Electrical Measurement – Online Delivery. Australia NMI. This course covers essential knowledge of the theory and practice of electrical measurement using digital multimeters and calibrators; special attention is given to important practical issues such as grounding, interference and thermal effects. https://shop.measurement.gov.au/collections/physical-metrology-training

SEMINARS & WEBINARS: General

Dec 9, 2020 Calibration and Measurement Fundamentals – Online Delivery. Australia NMI. This course covers general metrological terms, definitions and explains practical concept applications involved in calibration and measurements. The course is recommended for technical officers and laboratory technicians working in all industry sectors who are involved in making measurements and calibration process. https://shop.measurement.gov.au/collections/physical-metrology-training

SEMINARS & WEBINARS: Industry Standards

Nov 9-12, 2020 Understanding ISO/IEC 17025:2017 for Testing & Calibration Laboratories. Virtual. A2LA WorkPlace Training. This course is a comprehensive review of the philosophies and requirements of ISO/IEC 17025:2017. The participant will gain an understanding of conformity assessment using the risks and opportunities-based approach. https://www.a2lawpt.org/events

Nov 16-18, 2020 Internal Auditing to ISO/IEC 17025:2017. Live Online. ANAB. Attendees of this 2.5-day training course will learn how to coordinate a quality management system audit to ISO/IEC 17025:2017 and collect audit evidence and document observations, including techniques for effective questioning and listening. https://anab.ansi.org/public-course-schedule

Dec 8-9, 2020 Understanding ISO/IEC 17025 for Testing and Calibration Labs. Webinar. International Accreditation Service®. To learn about ISO/IEC 17025 from one of its original authors. This 2-day Training Course examines structural components of the standard. Quality system and technical requirements are grouped in a manner that makes them clear and understandable. https://www.iasonline.org/training/ias-training-schedule/

CALENDAR

Dec 7-11, 2020 Lead Assessor Intensive Training (ISO/IEC 17025 or ISO/IEC 17020). Live Online. ANAB has redesigned its Lead Assessor Intensive Training course to an exercise-based approach to better support and develop the competencies required of a lead assessor. The course was developed in response to the recent change of focus on competence within laboratory-related accreditation standards. https://anab.ansi.org/public-course-schedule

Dec 14-18, 2020 Forensic ISO/IEC 17025:2017 Internal Auditor. Live Online. ANAB. This course provides a detailed review of ISO/IEC 17025:2017 and the related ANAB accreditation requirements for forensic service providers (AR 3125) as well as a review of ISO 19011, Guidelines for Auditing Management Systems. https://anab.ansi.org/training/public-course-schedule

Jan 26-29, 2021 Lead Assessor Intensive Training (ISO/IEC 17025 or ISO/IEC 17020). Live Online. ANAB. ANAB has redesigned its Lead Assessor Intensive Training course to an exercise-based approach to better support and develop the competencies required of a lead assessor. The course was developed in response to the recent change of focus on competence within laboratory-related accreditation standards. https://anab.ansi.org/public-course-schedule

Feb 8-10, 2021 Internal Auditing to ISO/IEC 17025:2017. Live Online. ANAB. Attendees of this 2.5-day training course will learn how to coordinate a quality management system audit to ISO/IEC 17025:2017 and collect audit evidence and document observations, including techniques for effective questioning and listening. https://anab.ansi.org/public-course-schedule

Feb 22-26, 2021 Forensic ISO/IEC 17025:2017 Internal Auditor. Live Online. ANAB. This course provides a detailed review of ISO/IEC 17025:2017 and the related ANAB accreditation requirements for forensic service providers (AR 3125) as well as a review of ISO 19011, Guidelines for Auditing Management Systems. https://anab.ansi.org/training/public-course-schedule

Apr 26-30, 2021 Lead Assessor Intensive Training (ISO/IEC 17025 or ISO/IEC 17020). Washington, DC. ANAB has redesigned its Lead Assessor Intensive Training course to an exercise-based approach to better support and develop the competencies required of a lead assessor. The course was developed in response to the recent change of focus on competence within laboratory-related accreditation standards. https://anab.ansi.org/public-course-schedule

May 17-19, 2021 Internal Auditing to ISO/IEC 17025:2017. Washington, DC. ANAB. Attendees of this 2.5-day training course will learn how to coordinate a quality management system audit to ISO/IEC 17025:2017 and collect audit evidence and document observations, including techniques for effective questioning and listening. https://anab.ansi.org/public-course-schedule

May 17-20, 2021 Forensic ISO/IEC 17025:2017 Internal Auditor. Cary, NC. ANAB. This course provides a detailed review of ISO/IEC 17025:2017 and the related ANAB accreditation requirements for forensic service providers (AR 3125) as well as a review of ISO 19011, Guidelines for Auditing Management Systems. https://anab.ansi.org/training/public-course-schedule

SEMINARS & WEBINARS: Management & Quality

Feb 24-25, 2021 Documenting Your ISO/IEC 17025 Management System. Webinar. A2LA WorkPlace Training. During this course, the participant will gain an understanding of the basic concepts of management system documentation structure, content, and development. https://www.a2lawpt.org/events

SEMINARS & WEBINARS: Measurement Uncertainty

Nov 18-20, 2020 Introduction to Estimating Measurement Uncertainty – Online Delivery. Australia NMI. This one-day introductory course will give you the grounding needed to develop an uncertainty budget. Suitable for staff from calibration laboratories and those testing laboratories carrying out physical measurements, the course will give you a clear step-by-step approach to uncertainty estimation with practical examples. https://shop.measurement.gov.au/collections/physical-metrology-training

Nov 19-20, 2020 Fundamentals of Measurement Uncertainty. Live Online. ANAB. Attendees of the two-day Fundamentals Measurement Uncertainty training course will learn a practical approach to measurement uncertainty applications, based on fundamental practices. https://anab.ansi.org/public-course-schedule

Dec 7-8, 2020 Introduction to Measurement Uncertainty. Webinar. A2LA WorkPlace Training. This course is a suitable introduction for both calibration and testing laboratory participants, focusing on the concepts and mathematics of the measurement uncertainty evaluation process. https://www.a2lawpt.org/events/

Dec 10-11, 2020 Uncertainty of Measurement for Labs. Webinar. International Accreditation Services®. Introduction to metrology principles, examples and practical exercises. The training includes case studies and discussions, with application of statistical components in practical examples that are frequently encountered by testing laboratories. https://www.iasonline.org/training/

Jan 19, 2021 Introduction to Measurement Uncertainty. Webinar. A2LA WorkPlace Training. This course is a suitable introduction for both calibration and testing laboratory participants, focusing on the concepts and mathematics of the measurement uncertainty evaluation process. https://www.a2lawpt.org/events/

Feb 11-12, 2021 Fundamentals of Measurement Uncertainty. Live Online. ANAB. Attendees of the two-day Fundamentals Measurement Uncertainty training course will learn a practical approach to measurement uncertainty applications, based on fundamental practices. https://anab.ansi.org/public-course-schedule

Mar 8, 2021 Introduction to Measurement Uncertainty. Webinar. A2LA WorkPlace Training. This course is a suitable introduction for both calibration and testing laboratory participants, focusing on the concepts and mathematics of the measurement uncertainty evaluation process. https://www.a2lawpt.org/events/

Mar 9-10, 2021 Applied Measurement Uncertainty for Calibration Laboratories. Webinar. A2LA WorkPlace Training. During this course, the participant will be introduced to several tools and techniques that can be applied in the calibration laboratory to create measurement uncertainty budgets which comply with ISO/IEC 17025 requirements. https://www.a2lawpt.org/events

JOFRA calibration
Our dry-block and liquid bath portable temperature calibrators include 5 series with more than 25 models and temperature ranges from -100 to 1205° C. All feature portability, accuracy, speed, and advanced documenting functions with JofraCal calibration software. Our calibrators include the smallest and coldest dry-block temperature calibrator available. We can even provide special insert support for the most demanding job.
RTC-159
CTC-652
RTC-187
RTC-158
RTC-159
■ Ultra Cooler down to -100° C
RTC-187
■ Our Hottest Cold Temperature Calibrator
RTC-158
■ Combination Liquid Bath and Dry Block Calibration
CTC-652
■ 190 mm Immersion Depth for Long Sensors
AMETEK
SENSORS, TEST & CALIBRATION
ametekcalibration.com

May 20-21, 2021 Fundamentals of Measurement Uncertainty. Washington, DC. ANAB. Attendees of the two-day Fundamentals Measurement Uncertainty training course will learn a practical approach to measurement uncertainty applications, based on fundamental practices. https://anab.ansi.org/public-course-schedule

SEMINARS & WEBINARS: Pressure

Jun 23-24, 2021 Pressure Measurement. Port Mebourne, VIC. Australia NMI. This two-day course (9 am to 5 pm each day) covers essential knowledge of the calibration and use of a wide range of pressure measuring instruments, their principles of operation and potential sources of error — it incorporates extensive hands-on practical exercises. https://shop.measurement.gov.au/collections/physical-metrology-training

SEMINARS & WEBINARS: RF & Microwave

May 4-6, 2021 VNA Tools Training Course. Federal Institute of Metrology METAS. Bern-Wabern, Switzerland. VNA Tools is a free software developed by METAS for measurements with the Vector Network Analyzer (VNA). The software facilitates the tasks of evaluating measurement uncertainty in compliance with the ISO-GUM and vindicating metrological trace-ability. The software is available for download at www.metas.ch/vnatools. The three day course provides a practical and hands-on lesson with this superior and versatile software. https://www.metas.ch/metas/en/home/dl/kurse---seminare.html

SEMINARS & WEBINARS: Software

Nov 16-20, 2020 TWB 1051 MET/TEAM® Basic Web-Based Training. Fluke Calibration. This web-based course presents an overview of how to use MET/TEAM® Test Equipment and Asset Management Software in an Internet browser to develop your asset management system. http://us.flukecal.com/training

SEMINARS & WEBINARS: Temperature & Humidity

Nov 13, 2020 Testing Temperature Controlled Enclosures. Port Melbourne VIC, Australia. NMI. This one day course (9 am to 5 pm) is for people involved in routine performance testing of temperature controlled enclosures (oven, furnace, refrigerator and fluid bath). It incorporates an extensive overview of AS 2853 requirements and common industry practice and it also includes hands-on practical demonstrations. https://www.industry.gov.au/client-services/training-and-assessment

CALENDAR

Dec 15, 2020 Humidity Measurement – Online Delivery. Australia NMI. This course provides information about the main concepts and practical techniques involved in measuring humidity in air and explains how to make such measurements accurately and consistently. https://shop.measurement.gov.au/collections/physical-metrology-training

Mar 23-25, 2021 Temperature Measurement. Malaga WA, Australia. NMI. This three-day course (9 am to 5 pm) covers the measurement of temperature and the calibration of temperature measuring instruments. It incorporates extensive hands-on practical exercises. https://www.industry.gov.au/client-services/training-and-assessment

May 10, 2021 Temperature Measurement and Calibration (with optional practical day). Teddington, UK. NPL. This is a 2-3 day course, covering the range –200 °C to 3000 °C, the course will concentrate on those methods of measurement which are of greatest technological and industrial importance. https://training.npl.co.uk/course/temperature-measurement-and-calibration-with-optional-practical-day/

May 13, 2021 Humidity Measurement and Calibration. Teddington, UK. NPL. This is a 2 day course covering dew point, relative humidity and other humidity quantities, the course will concentrate on methods of measurement which are of greatest technological relevance to attendees. https://training.npl.co.uk/course/humidity-measurement-and-calibration/

SEMINARS & WEBINARS: Vibration

Jan 5-7, 2021 Fundamentals of Random Vibration and Shock Testing. Webinar. Equipment Reliability in collaboration with WESTPAK. Review basic vibrations, sources and causes, then explore vibration measurements, analysis and calibration. Our discussion is supported by projected visuals and video clips. We'll compare sinusoidal vs. random vibration with emphasis on testing systems, specifications, standards and procedures. https://equipment-reliability.com/open-courses/

Visit **www.callabmag.com** for upcoming metrology events & webinars!

ONLINE & INDEPENDENT STUDY

CERTIFICATIONS

AC/DC Metrology. A2LA WPT. This self-directed online course is an overview of AC/DC metrology, with a specific focus on preparing the learner for the CCT (Certified Calibration Technician) exam. https://www.a2lawpt.org/e-learning

Certified Calibration Technician Certification Preparation - Web-Based. ASQ. This self-paced course covers the material you will see on the CCT exam. It includes a practice test based on the CCT Body of Knowledge. https://asq.org/training/catalog

Certified Calibration Technician Exam Prep. A2LA WPT. This self-directed online course was designed to prepare the learner for the CCT (Certified Calibration Technician) exam, and covers the primary topics represented in the exam. https://www.a2lawpt.org/e-learning

Certified Calibration Technician Prep – Online. QC Training. Students prepare to take the ASQ's Certified Calibration Technician (CCT) exam. This course follows the ASQ body of knowledge with audio/visual presentations of the various topics to prepare the student for the CCT exam. https://qctraininginc.com/course/certified-calibration-technician-prep-online/

Certified Calibration Technician Question Bank - Web-Based. ASQ. Build confidence as you prepare for the ASQ CCT exam with hundreds of practice questions from ASQ. Simulate a timed exam from the convenience of your home or office, or review specific topic areas and identify your strengths and weaknesses. https://asq.org/training/catalog

DIMENSIONAL

Basic Dimensional Measurement Tools – Self Directed Learning. QC Training. This DVD course forms the basis for mastering more advanced measuring tasks to ensure that you'll get the accurate measurements needed for all data-based improvement efforts. https://qctraininginc.com/course/basic-dimensional-measurement-tools-self-directed-learning/

Coordinate Measuring Machine (CMM). A2LA WPT. This self-directed online course examines the basic concepts and principles of Coordinate Measuring Machines (CMMs), as defined by different manufacturers as well as the standard documents accepted by industry. https://www.a2lawpt.org/e-learning

Coordinate Measuring Machine Basics – Online. QC Training. This entry level course describes the CMM for the individual with limited to no knowledge of CMMs. Course content includes history of the CMM, basic terminology, specifications, standards, accuracy, and measurement uncertainty. https://qctraininginc.com/course/coordinate-measuring-machine-cmm-basics-online/

Dimensional Measurement User – E-learning. National Physical Laboratory. In this training course, learners will be introduced to dimensional metrology and the importance of good measurement practice. https://training.npl.co.uk/course/dimensional-measurement-user/

Geometric Dimensioning and Tolerancing (GD&T). A2LA WPT. This self-directed online course is an overview of Geometric Dimensioning and Tolerancing (GD&T) and is designed to give calibration technicians a general understanding of the history, applications, limitations, and use of GD&T. https://www.a2lawpt.org/e-learning

Level II Dimensional Measurement: Hardness. A2LA WPT. Participants in this self-directed online course will gain an advanced understanding of precision dimensional measurement relating to hardness. https://www.a2lawpt.org/e-learning

Level II Dimensional Measurement: Roundness. A2LA WPT. Participants in this self-directed online course will gain an advanced understanding of precision dimensional measurement relating to roundness. https://www.a2lawpt.org/e-learning

Level II Dimensional Measurement: Surface Texture. A2LA WPT. Participants in this self-directed online course will gain an advanced understanding of precision dimensional measurement relating to surface texture. https://www.a2lawpt.org/e-learning

Precision Dimensional Measurement. A2LA WPT. This Level I course covers the following precision dimensional measurement equipment as well as its usage and associated measurement principles: Gages/Gage Blocks, Interferometers, Optical Instruments. https://www.a2lawpt.org/e-learning

Precision Dimensional Measurement – Online. QC Training. Advance your career with a low-cost, online course in precision dimensional measurement, tools and techniques. https://qctraininginc.com/

ELECTRICAL

AC-DC Metrology– Self-Paced Online Training. Fluke Calibration. Learn the basic concepts of ac/dc metrology, including the theory and application of thermal transfer standards to measure ac voltages and currents, definition of inductance and capacitance, and the measurement of impedance, admittance and immittance. https://us.flukecal.com/training

Electrical Instrumentation for Applied Measurements – OnDemand Internet Course. Technology Training, Inc. (TTI). This course provides a basic understanding of electrical measurement systems, as well as the engineering concepts for the whole measurement system. https://ttiedu.com/

Precision Electrical Measurement. A2LA WPT. This Level I course covers the following precision electrical measurement equipment as well as its usage and associated measurement principles: Analog Meters, Digital Multi-Meters, Faraday Shields. https://www.a2lawpt.org/e-learning

Precision Electrical Measurement – Self-Paced Online Training. Fluke Calibration. Making precision measurements is a skill that takes practice and experience to master. This course will increase your knowledge of terminology, concepts and procedures to help you become more proficient. https://us.flukecal.com/training

FLOW

Introduction to Pipettes. A2LA WPT. This Level I course covers the following types of pipettes as well as their usage, applications, and associated measurement principles: Positive Air Displacement, Single Volume, Adjustable, and Multichannel Pipettes. https://www.a2lawpt.org/e-learning

Precision Flow Measurement. A2LA WPT. This Level I course covers precision flow measurement equipment as well as its usage and associated measurement principles. https://www.a2lawpt.org/e-learning

FORCE & TORQUE

Precision Force & Torque Measurement. A2LA WPT. This Level I course covers the following precision force and torque measurement equipment as well as its usage and associated measurement principles: Transducers, Load Cells, Proving Rings, Torque Testers. https://www.a2lawpt.org/e-learning

GENERAL

Basic Measurement Concepts Program. Learning Measure. This program introduces basic measurement concepts, the SI system of units, and measurement uncertainty analysis. http://www.learningmeasure.com/programs.shtml

Calibration Laboratory Operations – OnDemand Internet Course. Technology Training, Inc. (TTI). This course is for individuals who are involved in standards and calibration laboratories and for others who want a clear understanding of the special requirements that must be met by managers and other personnel in standards and calibration work. https://ttiedu.com/

Career Long Learning. Sine Calibration School. Our full curriculum starts with the Basic Calibration Course. From there, you can continue to learn with yearly courses in various calibration subjects to further your calibration understanding and knowledge. https://www.sinecalibrationschool.com/

Fundamentals of Calibration. Sine Calibration School. Our full curriculum starts with the Basic Calibration Course. From there, you can continue to learn with yearly courses in various calibration subjects to further your calibration understanding and knowledge. https://www.sinecalibrationschool.com/

Instrumentation for Test and Measurement – OnDemand Internet Course. Technology Training, Inc. (TTI). Course 163 presents basic information on selection, application, calibration and usage of modern measurement systems to measure electrical, environmental and dynamic phenomena. https://ttiedu.com/

Interval Analysis. A2LA WPT. This self-directed online course focuses on concepts associated with calibration intervals and interval analysis, specifically to determine the correct calibration interval necessary to maintain measurement quality over a time interval. https://www.a2lawpt.org/e-learning

ONLINE & INDEPENDENT STUDY

Introduction to Analytical Measurement. A2LA WPT. This course introduces analytical measurement concepts that lay the foundation for a variety of analytical industry segments, including chemical, biotechnology, environments, and forensics. It covers relevant mathematics, common error sources, the operation of principle measurement, devices, and further key concepts. https://www.a2lawpt.org/e-learning

Introduction to Measurement and Calibration. A2LA WPT. This self-directed online course is an overview of measurement and calibration principles, starting with the purpose of metrology and the concepts associated with accuracy, error, bias and measurement uncertainty. https://www.a2lawpt.org/e-learning

Introduction to Measurement and Calibration – Self-Paced Online Classes. Fluke Calibration. This course instructs the user on basic concepts of measurement and calibration. https://us.flukecal.com/training

Introduction to Measurement and Calibration - Web-Based. ASQ. Satisfy the requirements for ISO 17025 and 16949, FDA, and FAA. You will learn skills including standardization, managing a metrology system, and units and instrumentation of measurements. https://asq.org/training/catalog

Introduction to Metrology - e-Learning. National Physical Laboratory. This half-day, certified e-learning course has been designed to introduce metrology and explore its value for industry, the economy, science and society. https://training.npl.co.uk/course/introduction-to-metrology/

Measurement and Calibration Overview – Online Training. QC Training. This course is an introduction to the topics of measurement and calibration designed to give the student a general overview of the subject. https://qctraininginc.com/course/introduction-to-measurement-calibration-online/

Measurement Fundamentals Explained – e-Learning. National Physical Laboratory. This unit introduces metrology, along with some basic metrology concepts. This free course is the ideal precursor to our more extensive, certified, Introduction to Metrology e-Learning course. https://training.npl.co.uk/course/measurement-fundamentals-explained/

Measurements Overview (QIMT1200) – Online Metrology Courses. Quametec. A parallel series of courses, which provide an introduction to, and description of, typical measurements performed in the dimensional, physical and electrical disciplines in science and industry. https://www.qimtonline.com

Metrology Applications for Engineers and Scientists. A2LA WPT. This self-directed online course is designed to familiarize engineers and scientists with metrology, the science of measurement, as it applies to their respective disciplines. https://www.a2lawpt.org/e-learning

Metrology Applications for Engineers and Scientists – Web-based. ASQ. When completed, you'll have a proper understanding of metrology concepts, basic statistics, reliability statistics and measurement uncertainty. https://asq.org/training/metrology-applications-for-engineers-and-scientists-metappwpt

Metrology Concepts – OnDemand Internet Course. Technology Training, Inc. (TTI). Provides a basic understanding of the wide range of activities encompassed by personnel working in standards and calibration laboratories. https://ttiedu.com/

Proficiency Testing. A2LA WPT. This self-directed online course covers information that laboratory management personnel need to conduct a better measurement assurance program and improve the outcome of proficiency testing. https://www.a2lawpt.org/

Safety in the Calibration Lab. A2LA WPT. This self-directed online course provides an understanding of potential hazards present in the calibration lab and how to mitigate risk by applying proper safety measures. https://www.a2lawpt.org/e-learning

Test Instruments Operation and Calibration. A2LA WPT. This is a general overview of the principles and best practices associated with operating and calibrating test instruments. https://www.a2lawpt.org/e-learning

INDUSTRY STANDARDS

Assessment to the Requirements of ISO/IEC 17025. A2LA WPT. This self-directed online course provides a comprehensive look at ISO/IEC 17025:2017 and its requirements from an auditing perspective. https://www.a2lawpt.org/e-learning

Assessment to the Requirements of ISO/IEC 17025 – Web-based. ASQ. This course is targeted toward management and what they need to be conformant to the standard. Learn about the requirements of the standard, how to prepare for the audit, how to conduct an audit of calibration suppliers. https://asq.org/training/

Changes to ISO/IEC 17025:2017. IAS. The course will present the major new changes to ISO/IEC Standard 17025. https://www.iasonline.org/training/ias-online-training-now-available/

How to Calculate Calibration Uncertainty in Accordance with ILAC P14. ISOBudgets. This course is going to teach you how to calculate and report measurement uncertainty in your calibration reports, based on the requirements of ISO/IEC 17025:2017 and

ILAC P14:01/2013. https://www.isobudgets.com/courses/

Introduction to ISO/IEC 17025 for Technicians. A2LA WPT. This self-directed online course focuses on the requirements of ISO/IEC 17025, how it is applied to calibration and test laboratories, and identified key information for technicians who work in an accredited lab. https://www.a2lawpt.org/e-learning

ISO/IEC 17025 Compliance – Web-based. ASQ. Understand the terminology, concepts, and procedures relating to ISO 17025 compliance and uncertainty management. This self-paced online course is ideal for Calibration Coordinators, Calibration Technicians and Engineers, and Quality Coordinators. https://asq.org/training/

ISO/IEC 17025 for Laboratories. IAS. This 2-day Training Course examines structural components of the standard. Quality system and technical requirements are grouped in a manner that makes them clear and understandable. https://www.iasonline.org/training/ias-online-training-now-available/

ISO/IEC Conformance: Uncertainty Management. A2LA WPT. This self-directed online course provides a detailed perspective on the concept of uncertainty management as it pertains to ISO/IEC 17025. https://www.a2lawpt.org/e-learning

MASS

Basic Mass Computer-Based Training. NIST OWM. Free download available in English and Spanish. https://www.nist.gov/pml/weights-and-measures/laboratory-metrology/lab-metrology-training

Precision Mass Measurement. A2LA WPT. This Level I course covers precision mass measurement equipment as well as its usage and associated measurement principles. https://www.a2lawpt.org/e-learning

MEASUREMENT UNCERTAINTIES

How to Calculate Measurement Uncertainty for ISO/IEC 17025. ISOBudgets. In this course, you will learn much more than just theory! Learn the tactics to calculate uncertainty, so you can confidently estimate uncertainty and impress your auditors. https://www.isobudgets.com/courses/

How to Calculate Measurement Uncertainty in Chemistry per EURACHEM/CITAC CG4 Guide. ISOBudgets. Learn how to estimate uncertainty in chemistry for ISO/IEC 17025:2017 accredited testing labs. This course is best suited for chemical testing labs that use HPLCs, GCs, and MS. https://www.isobudgets.com/courses/

ONLINE & INDEPENDENT STUDY

Introduction to Measurement Uncertainty – e-Learning. National Physical Laboratory. This half day, certified e-learning course explores measurement uncertainty and related concepts. https://training.npl.co.uk/course/introduction-to-measurement-uncertainty/

Measurement Uncertainty. A2LA WPT. This self-directed online course is designed to instruct and evaluate the user on concepts of measurement uncertainty. https://www.a2lawpt.org/e-learning

Measurement Uncertainty – OnDemand Internet Course. Technology Training, Inc. (TTI). Course 132 begins with an introduction to measurement uncertainty and to the terms associated with it. Then the accuracy and limitations of statistics are discussed, with examples of the various types of distributions encountered in statistical tests. https://ttiedu.com/

Measurement Uncertainty – Self-Paced Online Training. Fluke Calibration. Learn the fundamental concepts and how to successfully determine measurement uncertainty and quality improvement techniques. https://us.flukecal.com/training

Measurement Uncertainty – Web-based. ASQ. The focus of making quality measurements is to reduce uncertainty where possible, and to increase confidence in the measurements results in design, manufacturing, or quality in the aerospace, medical device, automotive industry or a calibration laboratory. https://asq.org/training/catalog

Measurement Uncertainty Analysis – Online Training. QC Training. This course is an introductory presentation about Measurement Uncertainty concepts and calculations required of most calibration and testing laboratories accredited to ISO standards. https://qctraininginc.com/

Measurement Uncertainty Analysis (QIMT1410) – Online Metrology Course. Quametec. This course takes the student through the basics of the ISO GUM to advanced concepts and methods designed to enable the student to perform measurement uncertainty analyses with confidence. https://www.qimtonline.com

Measurement Uncertainty Explained – e-Learning. NPL. This free course will provide an introduction to the concept and importance of measurement uncertainty and demonstrate the basics of uncertainty evaluation in eight steps. https://training.npl.co.uk/course/measurement-uncertainty-explained/

The Uncertainty Analysis Program. Learning Measure. This program covers all the courses concerning uncertainty and uncertainty analysis. http://www.learningmeasure.com/programs.shtml

Understanding Uncertainty Budgets – e-Learning. National Physical Laboratory. This course teaches measurement uncertainty through practical examples of uncertainty budgets. https://training.npl.co.uk/course/understanding-uncertainty-budgets/

PRESSURE & VACUUM

Precision & Vacuum Measurement. A2LA WPT. This Level I course covers the following precision pressure and vacuum measurement equipment as well as its usage and associated measurement principles: Transducers, Pressure Measurement Devices. https://www.a2lawpt.org/e-learning

RF & MICROWAVE

Basic Antenna Measurement Program. Learning Measure. This program covers concepts associated with basic antenna measurements. http://www.learningmeasure.com/programs.shtml

Basic RF & Microwave Program. Learning Measure. This is an introductory program covering the RF and microwave measurement field. http://www.learningmeasure.com/programs.shtml

Keysight RF & Microwave Fundamentals eLearning Program. Keysight Technologies. Build a strong foundation in RF & microwave fundamentals. https://www.keysight.com/find/rffundamentals

Microwave Principles. A2LA WPT. This self-directed online course provides an overview of microwave and radiofrequency microelectronics systems of all sizes and types, their applications, and the measurement and calibration principles associated with them. https://www.a2lawpt.org/e-learning

RF Measurement, Calibration and Connector Care. A2LA WPT. This self-directed online lesson describes principles and background information for the measurement of radio frequency electromagnetic fields. https://www.a2lawpt.org/e-learning

TEMPERATURE

Precision Humidity Measurement. A2LA WPT. This Level I course covers Hygrometers, Chilled Mirror Hygrometers, Wet and Dry Bulb Psychrometers, as well as their usage and associated measurement principles. https://www.a2lawpt.org/e-learning

Precision Temperature Measurement. A2LA WPT. This Level I course covers Thermocouples, Resistance Temperature Detectors, Thermistors, Infrared Sensor, including usage and associated measurement principles. https://www.a2lawpt.org/e-learning

TIME & FREQUENCY

Time and Frequency Measurement. A2LA WPT. This self-directed online course is an overview of the basic concepts of time and frequency measurement, as they apply to a wide range of disciplines. https://www.a2lawpt.org/e-learning

VIBRATION

Acoustics and Vibration Measurement. A2LA WPT. This self-directed online course will enable calibration technicians to precisely and reliably measure acoustics and vibration in accordance with relevant ISO standards. https://www.a2lawpt.org/e-learning

Fixture Design for Vibration and Shock Testing – OnDemand Internet Course. Technology Training, Inc. (TTI). Course 157 starts with a basic introduction to shakers and vibration testing. General considerations in fixture design are discussed next, along with an introduction to instrumentation and sinusoidal vibration testing, as they apply to the fixture design and evaluation process. https://ttiedu.com/

ISO 9001:2015 / AS9100D / CMMI Level III

KIHOMAC

POSITIONS AVAILABLE

Test & Measurement Engineering

KIHOMAC is currently seeking mid-career level software and hardware engineering professionals and technical leaders for our team.

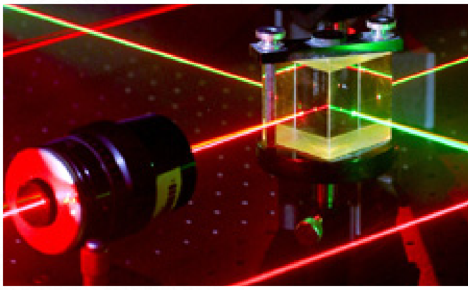

In aerospace and defense, *technology* is the platform, and KIHOMAC delivers it. Come and join our team supporting Naval Aviation weapon system acquisition, research, development, test, and evaluation.

We offer competitive salaries, outstanding benefits, and a customer oriented, positive and authentic culture. Our medical, dental, and vision coverage are first rate with low employee contributions.

PATUXENT RIVER OFFICE

Positions are currently available at our Southern Maryland office. Enjoy everything Maryland has to offer including 3,000 miles of coastline, early American history, boating, fishing, sports, entertainment and some of the best seafood in the country.

If you're looking for a fast-paced, high-tech position supporting essential missions, send a copy of your resume to TA@kihomac.com

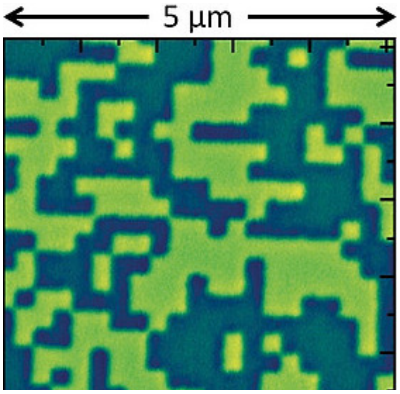

Test sample with magnetic structures used for the measurements performed within the scope of the interlaboratory comparison. The light green areas consist of a magnetic layer; in the darker areas, this layer was removed by means of lithography.

Reliable Measurement of Magnetic Fields on the Nanometer Scale

PTB News 2.2020 – So far, no internationally standardized measurement procedures have been available to measure magnetic field distributions that vary spatially on the nanometer scale. The *NanoMag* EMPIR metrology research project, which was spearheaded by PTB and has recently been completed with success, bridges this gap and will allow internationally comparable measurements of magnetic field distributions with high spatial resolution.

To further develop magnetic system components such as sensors and magnetic memories, industry needs traceable magnetic field measuring systems with the best possible spatial resolution. Magnetic field measurement procedures can be traced to a quantum standard by means of nuclear resonance and are well established, but so far, measurement procedures with spatial resolution could only be used qualitatively or for relatively large structures.

The partners of the recently completed *NanoMag* project have therefore developed several procedures with high spatial resolutions, elaborated calibration procedures and made reference materials available for calibration.

One of the most relevant project results was that it had been the first time that measurement procedures for magnetic field distributions traceable to the SI with the highest possible spatial resolutions of down to 10 nm had been developed, tested and validated by an international interlaboratory comparison. Within the scope of this comparison – with the participation of PTB – measurement data of magnetic force microscopes were successfully compared with each other in the field range around 0.1% T.

For one thing, this has laid the foundations for a corresponding measurement infrastructure at the three European metrology institutes involved in the research project. For another, an IEC standard on the spatially resolved measurement of magnetic field distributions has been developed based on the results. This standard will allow reliable and internationally comparable quantitative nanomagnetic measurements.

Additional information: https://www.ptb.de/empir/nanomag.html

Source: https://www.ptb.de/cms/en/presseaktuelles/journals-magazines/ptb-news.html

Researchers to Streamline Process for Measuring Aviation Emissions

Posted by Delia Croessmann on July 9, 2020 – The process that airlines must use to calibrate their jet fuel emissions measuring systems is costly and time-consuming. But researchers at Missouri S&T won an $847,000 Federal Aviation Administration (FAA) grant to find a faster and less expensive way to calibrate the devices.

To reduce the impact of civil aviation on local air quality and human health, the International Civil Aviation Organization (ICAO) has established and continually improved emissions standards for turbojet and turbofan engine emissions since 1981. To address a gap in the existing standards, the ICAO Council recently adopted a new non-volatile particulate matter (nvPM) emission standard that will govern both new and in-production engines from 2023 onward.

"The ICAO conducts an unbelievably rigorous evaluation process to certify commercial jet engines for safety and climate-related regulations," says Dr. Philip Whitefield, Chancellor's Professor and professor emeritus of chemistry at Missouri S&T. "But the time and expense of calibrating emissions measuring systems, which have to be highly accurate and precise, is a component of the certification process that warrants improvement."

To meet certification requirements, engine manufacturers must ship certain components of their emissions measuring devices to the device manufacturer—some of which are abroad—for an annual calibration process that can take two to three months and may cost as much as $25,000 per calibration, Whitefield says.

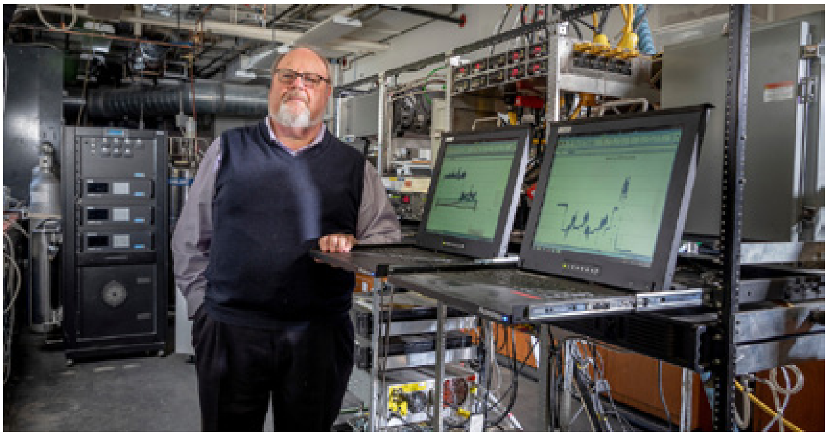

Dr. Philip Whitefield, Chancellor's Professor and professor emeritus of chemistry at Missouri S&T, with S&T's North American Reference System (NARS) used for engine emissions measurement. Photo by Tom Wagner, Missouri S&T. Permission granted by Missouri S&T for reprint.

Measurements International

Metrology is Our Science, Accuracy is Our Business™

NEW PRODUCT ANNOUNCEMENTS

1310A AUTOMATED RESISTANCE STANDARD

Simplify Your Procedures.
Simplify Your Work.

- ► 9 Resistors: 1 Ω to 100 MΩ plus 1 External Channel
- ► Front Panel or GPIB Controlled
- ► Single Output Cable for Direct Plug-in

1330A AUTOMATED ARTIFACT CALIBRATOR

Three Standards – One Box

- ► Primary 1 Ω, 10 kΩ and 10 V References
- ► Direct Plug-in Cable to 57XXA or 8.5 Digit DVM Terminals
- ► Battery Backup Option > 72 Hours

1340A HIGH PRECISION VOLTAGE DIVIDER

Developed & designed BY metrologists FOR metrologists & calibration technicians

- ► 1000:1, 100:1, 10:1 Divider Outputs
- ► Voltages to 1000 Volts
- ► No Self-Alignment Required

Measurements International Ltd.,
PO Box 2359,
118 Commerce Drive,
Prescott, Ontario, Canada
K0E 1T0

1-800-324-4988

sales@mintl.com

http://www.mintl.com

Whitefield and his research team want to find a faster and less costly way to capture the jet engines' nvPM measurements. He is the principal investigator on the grant to develop a user-friendly calibration source that will characterize and quantify jet engine emissions onsite at the certification facilities on a more frequent basis and at a greatly reduced cost.

The team plans to synchronize the new measuring devices with the North American Reference System (NARS), an nvPM-measuring system Missouri S&T designed in collaboration with the Society of Automotive Engineers. Engine manufacturers throughout the U.S. and Canada now use NARS as a standard system. The prototype mass calibration devices will be tested along with the NARS at the U.S. Air Force Arnold Engineering Development Complex at Arnold Air Force Base in Tullahoma, Tennessee.

Whitefield's goal is for the ICAO to include the new calibration methodology in its updated certification standards, which are slated for release in 2023. He also envisions that other industries such as the automotive sector could use the methodology for emissions measurements.

Co-investigators on the project are Dr. Richard Miake-Lye of Aerodyne Research Inc. and Dr. Robert Howard of the U.S. Air Force Arnold Engineering Development Complex. Steven Achterberg, senior research specialist at Missouri S&T, is technical lead. Other research partners affiliated with the project include the U.S. Environmental Protection Agency, Transport Canada and the National Research Council Canada.

The FAA Air Transportation Center of Excellence for Alternative Jet Fuels and Environment (AJFE) award supports the project "Particulate Matter and Gas Phase Emissions Measurement of Aircraft Engine Exhaust" and is associated with in-kind cost share from EMPA, the Swiss Federal Laboratories for Material Science and Technology. The project is expected to be completed in June 2021.

Source: https://news.mst.edu/2020/07/researchers-to-streamline-process-for-measuring-aviation-emissions/

CAL-TOONS by Ted Green teddytoons@icloud.com

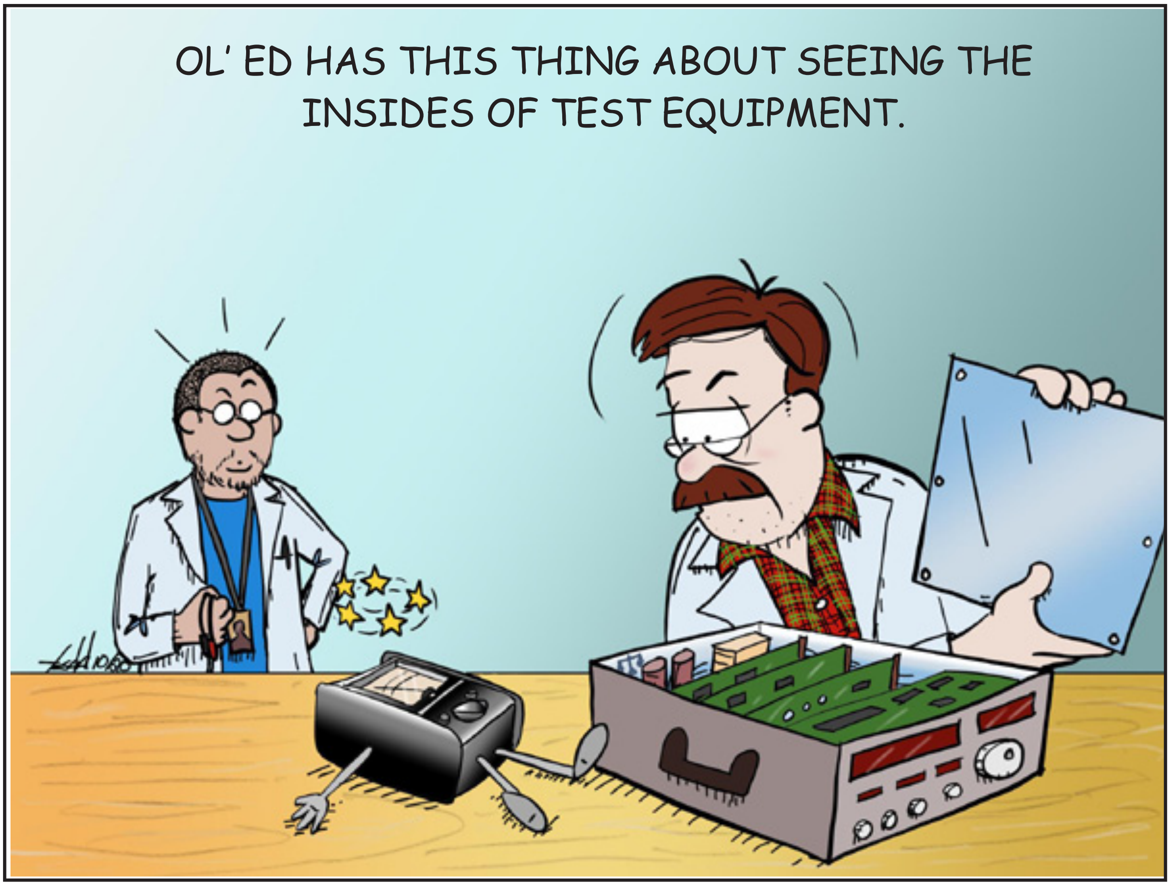

king nutronics corporation

RANGE
95-662°F (35-350°C)

ACCURACY
+/-0.25°F (0.14°C)

DIMENSIONS (WxHxD)
11" x 14" x 18"
(279 mm x 355 mm x 457 mm)

WEIGHT
15 lb (6.8 kg)

TAKE LABORATORY ACCURACY TO THE FIELD

REGULUS 4200 DUAL-POWER TEMPERATURE CALIBRATOR

The **Regulus 4200 Dual-Power Temperature Calibrator** sets new standards for accuracy and stability and comes packaged to take the abuse of field work.

Designed for portability and durability, the Regulus 4200 is precision-engineered to go where others cannot. The robust interface, compact size and revolutionary new well design equips technicians with a calibration solution they can take to any site or lab and rely on for many years. The patent-pending dual-power modulation blazes new trails for energy-efficiency by conserving power and reducing electricity draw.

Compact, tough, reliable and packed with new technology that saves energy and rewrites the definition of field metrology.

818.887.5460 | www.kingnutronics.com

Two Simple and Practical Methods for Combining Prior Information with Current Measurement in Uncertainty Analysis

Hening Huang
Teledyne RD Instruments, Retired

This paper presents two simple and practical frequentist methods for combining prior information with current measurement in uncertainty analysis. The first method is based on the "law of combination of distributions" (LCD). The second method is based on the least-squares principle. We focus on a problem that is often encountered in practice: the prior information is available from historical measurements and the current measurement gives a series of observations. Under the assumption of normality, both the LCD-based and least-squares methods give the same results. The philosophical and methodological difference between the LCD-based method and the Bayesian approach is discussed. This paper also presents a simple test to determine whether prior information is valid. If prior information is invalid, it should not be incorporated into current measurement because otherwise it would deteriorate the quality of the estimation of the measurand. Four examples are presented to demonstrate the effectiveness of the proposed frequentist methods, compared with their Bayesian counterparts.

1. Introduction

Consider that a physical quantity of interest is measured n times under the same measurement condition to give a series of observations. We assume that the observations, denoted by X, are randomly drawn from a normal distribution with mean μ and variance σ^2, i.e. $X \sim N(\mu, \sigma^2)$. In practice, μ is unknown (otherwise, there is no need to make measurements). We want to determine an appropriate estimator of μ, denoted by $\hat{\mu}$, and associated standard uncertainty (SU).

In the case that no prior information on the measurand is available, it is a common practice to use the sample mean $\bar{x}$ as an estimator of μ, i.e $\hat{\mu} = \bar{x}$. When σ is known (e.g. from manufacturer's specification), the SU of $\bar{x}$ is $\sigma/\sqrt{n}$ that is a Type B uncertainty according to the GUM (JCGM 2008); when σ is unknown, the SU is estimated as $\widehat{\mathrm{SU}} = \hat{\sigma}/\sqrt{n}$ that is a Type A uncertainty (where $\hat{\sigma}$ is an estimator of σ). It is important to note that $\mathrm{SU} = \sigma/\sqrt{n}$ is the scale parameter of the sampling distribution, and $\widehat{\mathrm{SU}}$ is an estimate of the SU based on a sample. Readers may refer to Huang (2020) for detailed discussion on the meaning of the standard uncertainty.

In practice, prior information on the measurand is sometimes available. For example, historical measurements may give a sample mean x_{prior} and variance $\sigma^2_{\mathrm{prior}}$. It is desirable to combine the prior information with the current measurement in the estimation of the measurand and associated uncertainty. Then, we need to answer two questions. The first question is: "how to incorporate prior information into current measurement?" The second question is: "how to determine whether prior information is valid?" The concern about the validity of a prior was raised by Phillips, Estler, Levenson, and Eberhardt in 1998. However, the concern has not been solved. If prior information is invalid (e.g. due to a change of measurement condition), it should not be incorporated into current measurement because otherwise it would deteriorate the quality of the estimation of the measurand.

It is well known that Bayesian statistics can provide mathematical methods for combining prior information with current measurement. A classical solution based on the Bayesian approach to the problem considered when σ is known is described in Appendix A. In general, however, Bayesian approaches are complicated in formulation and in numerical calculation, which most practitioners are not familiar with.

In contrast, it is rarely known whether frequentist statistics can provide mathematical methods for combining prior information with current measurement. In fact, it is a general perception that prior information can be incorporated only with the Bayesian framework.

The purpose of this study is to explore the possibility of combining prior information with current measurement with frequentist methods. It turns out that the combination can be made with two simple and practical frequentist methods. In the following, section 2 presents method 1 that is based on the "law of combination of distributions" (LCD). Section 3 presents method 2 that is based on the least-squares principle. Section 4 presents a simple test for the validity of a prior. Section 5 presents four examples. Sections 6 and 7 present discussion and conclusion respectively.

2. Method 1: LCD-based Method

2.1 The Proposed Formula

Frequentists view the unknown parameter μ as a fixed constant (i.e. the true value of the measured quantity). Thus, $X = \mu$ + error. We assume that the error is normally distributed. In the frequentist setting, we assume that there exist two "sampling" distributions of x. One is the sampling distribution with its parameters (location and scale parameters) estimated with point estimation, using the data collected (i.e. n observations). It is referred to as the current distribution (i.e. probability density function (PDF)), denoted by $p_{\text{current}}(x)$. The other is the distribution with its parameters given by the prior information (x_{prior} and σ^2_{prior}) based on historical measurements (or professional judgment). It is referred to as the prior distribution, denoted by $p_{\text{prior}}(x)$. We further assume that $p_{\text{prior}}(x)$ and $p_{\text{current}}(x)$ are independent. This is a reasonable assumption because a current measurement in general has nothing to do with a historical measurement. We want to combine the two distributions into one, referred to as posterior distribution, denoted by $p_{\text{post}}(x)$.

According to the law of combination of distributions (LCD) that is described in Appendix B, the posterior PDF of x can be written as

$$p_{\text{post}}(x) = \frac{p_{\text{prior}}(x) \cdot p_{\text{current}}(x)}{\int p_{\text{prior}} \cdot p_{\text{current}}(x)dx} \qquad (1)$$

An analytical solution to $p_{\text{post}}(x)$ may be available for some problems. For example, if both $p_{\text{prior}}(x)$ and $p_{\text{current}}(x)$ are Gaussian PDFs, $p_{\text{post}}(x)$ is also a Gaussian PDF. Otherwise, $p_{\text{post}}(x)$ can be determined using numerical discretization

$$p_{\text{post}}(x_i) = \frac{p_{\text{prior}}(x_i) \cdot p_{\text{current}}(x_i)}{\sum_{i=1}^{m} p_{\text{prior}}(x_i) \cdot p_{\text{current}}(x_i)} \qquad (2)$$

in which, the range of x is divided into m intervals.

It should be emphasized that Eq. (1) or (2) is derived entirely based on the frequentist view (i.e. the sampling theory and point estimation), it should not be interpreted with the Bayesian view. Further discussion on the philosophical and methodological difference between the proposed LCD-based method and the Bayesian approach will be given later in this paper.

2.2 When σ is Known

For the problem considered when σ is known, we assume that the prior distribution is normal with mean x_{prior} and variance σ^2_{prior}. That is

$$p_{\text{prior}}(x) = N(x_{\text{prior}}, \sigma^2_{\text{prior}}) \qquad (3)$$

The true current (measurement) distribution is $N(\mu, \frac{\sigma^2}{n})$. Since μ is unknown, we use the sample mean $\bar{x}$ as its estimate. Thus, the estimated current distribution $p_{\text{current}}(x)$ is

$$p_{\text{current}}(x) = N(\bar{x}, \frac{\sigma^2}{n}) \qquad (4)$$

According to Eq. (1), the posterior distribution $p_{\text{post}}(x)$ can be written as

$$p_{\text{post}}(x) \propto N(x_{\text{prior}}, \sigma^2_{\text{prior}}) \cdot N(\bar{x}, \frac{\sigma^2}{n}) \qquad (5)$$

Thus, $p_{\text{post}}(x)$ is also normal, $N(x_{\text{post}}, \sigma^2_{\text{post}})$. Consequently, x_{post} is an estimate of μ (denoted by $\hat{\mu}$) and the square root of σ^2_{post} is an estimate of SU (denoted by $\widehat{\text{SU}}$)

$$\hat{\mu} = \frac{\frac{x_{\text{prior}}}{\sigma^2_{\text{prior}}} + \frac{\bar{x}}{\sigma^2/n}}{\frac{1}{\sigma^2_{\text{prior}}} + \frac{1}{\sigma^2/n}} \qquad (6)$$

$$\widehat{\text{SU}} = \frac{1}{\sqrt{\frac{1}{\sigma^2_{\text{prior}}} + \frac{1}{\sigma^2/n}}} \qquad (7)$$

It can be recognized that $\hat{\mu}$ is an inverse-variance weighted-average (WA) (denoted by inverse-σ^2 WA hereafter) of the prior mean x_{prior} and the current (sample) mean $\bar{x}$. These results are the same as those given by the Bayesian approach, i.e. $\hat{\mu} = \hat{\mu}_{\text{SB}}$ and SU = SU_{SB} [refer to Appendix A].

2.3 When σ is Unknown

When σ is unknown, we employ $\hat{\sigma}$ as an estimate of σ. Accordingly, the estimated current distribution $p_{\text{current}}(x)$ is

$$p_{\text{current}}(x) = N\ (\bar{x}, \frac{\hat{\sigma}^2}{n}) \qquad (8)$$

Again, according to Eq. (1), the posterior distribution $p_{\text{post}}(x)$ becomes

$$p_{\text{post}}(x) \propto N(x_{\text{prior}}, \sigma^2_{\text{prior}}) \cdot N(\bar{x}, \frac{\hat{\sigma}^2}{n}) \qquad (9)$$

Thus, $p_{\text{post}}(x)$ is also normal. The estimators of μ and SU are written as

$$\hat{\mu} = \frac{\frac{x_{\text{prior}}}{\sigma^2_{\text{prior}}} + \frac{\bar{x}}{\hat{\sigma}^2/n}}{\frac{1}{\sigma^2_{\text{prior}}} + \frac{1}{\hat{\sigma}^2/n}} \qquad (10)$$

$$\widehat{\text{SU}} = \frac{1}{\sqrt{\frac{1}{\sigma^2_{\text{prior}}} + \frac{1}{\hat{\sigma}^2/n}}} \qquad (11)$$

Therefore, unlike the Bayesian approach that is unable to provide a solution to the problem considered when σ is unknown (refer to Appendix A), the proposed LCD-based method provides a reasonable, approximate solution.

3. Method 2: Least-squares Estimation

3.1 Formulation

We assume that the prior information x_{prior} and σ^2_{prior} describes the prior "sample"; $\bar{x}$ and $\hat{\sigma}^2/n$ describes the current sample. We define the normalized residual as the ratio between the residual and the standard deviation (Mohr and Taylor 2000, Huang 2018c, Merkatas et al. 2019). The sum of squares of the normalized residuals (SSNR) of the two samples is

$$\text{SSNR} = \left(\frac{x_{\text{prior}} - \hat{\mu}}{\sigma_{\text{prior}}}\right)^2 + \left(\frac{\bar{x} - \hat{\mu}}{\hat{\sigma}/\sqrt{n}}\right)^2 \tag{12}$$

The least -squares principle, i.e. the minimization of SSNR, is employed to determine $\hat{\mu}$

$$\frac{\partial\,(\text{SSNR})}{\partial\hat{\mu}} = \left(\frac{x_{\text{prior}} - \hat{\mu}}{\sigma^2_{\text{prior}}}\right) + \left(\frac{\bar{x} - \hat{\mu}}{\hat{\sigma}^2/n}\right) = 0 \tag{13}$$

Rearranging Eq. (13) to solve $\hat{\mu}$ gives an inverse-σ^2 WA that is the same as Eq. (10).

The conditional SU of $\hat{\mu}$ (Eq. (10)), conditioned on the prior and current samples, can be written as

$$\widehat{\text{SU}}_{\text{conditional}} = \frac{1}{\sqrt{\frac{1}{\sigma^2_{\text{prior}}} + \frac{1}{\hat{\sigma}^2/n}}} \tag{14}$$

It is important to note that $\widehat{\text{SU}}_{\text{conditional}}$ accounts for the within-sample variances, σ^2_{prior} and $\hat{\sigma}^2/n$, only; it does not account for the discrepancy between the two means or the heterogeneity between the two samples. It is intuitive that, if there is a significant discrepancy between x_{prior} and $\bar{x}$, the actual (unconditional) uncertainty of $\hat{\mu}$ will be large. Therefore, the conditional SU is valid only when the discrepancy between x_{prior} and $\bar{x}$ is small, or strictly speaking, the prior and current samples are drawn from the same parent distribution.

The author (Huang 2019a) presented a formula for estimating the unconditional SU of a WA based on a modification of the robust estimator of variance proposed by Sidik and Jonkman (2002). The formula is applicable to any type of weight w_j. It is written as

$$\widehat{\text{SU}}_{\text{unconditional}} = \frac{1}{c_4\sqrt{N-1}}\sqrt{\frac{\Sigma_{j=1}^{N} w_j\,(x_j - \hat{\mu})^2}{\Sigma_{j=1}^{N} w_j}} \tag{15}$$

where c_4 is a bias-correction factor for the sample standard deviation.

For the problem considered, N=2, c_4 =0.7979, x_1=x_{prior}, w_1=1/σ^2_{prior}, $x_2 = \bar{x}$, and $w_2 = 1/(\hat{\sigma}^2/n)$. The unconditional SU of $\hat{\mu}$ is written as

$$\widehat{\text{SU}}_{\text{unconditional}} = 1.25\sqrt{\frac{\frac{1}{\sigma_{\text{prior}}}(x_{\text{prior}} - \hat{\mu})^2 + \frac{1}{\hat{\sigma}/\sqrt{n}}(\bar{x} - \hat{\mu})^2}{\frac{1}{\sigma_{\text{prior}}} + \frac{1}{\hat{\sigma}/\sqrt{n}}}} \tag{16}$$

In principle, $\widehat{\text{SU}}_{\text{unconditional}}$ should be greater than $\widehat{\text{SU}}_{\text{conditional}}$ because it accounts for both the between-sample variance (i.e. squared residuals) and the within-sample variances. However, in the case where the squared residuals are near or equal to zero, $\widehat{\text{SU}}_{\text{unconditional}}$ may be smaller than $\widehat{\text{SU}}_{\text{conditional}}$. In fact, if $\widehat{\text{SU}}_{\text{unconditional}}$ < $\widehat{\text{SU}}_{\text{conditional}}$, it is most likely that the prior and current samples are drawn from the same parent distribution. That is, there is no heterogeneity between the two samples. In this situation, the unconditional SU estimator is inappropriate and the conditional SU estimator should be used.

3.2 Remarks

It should be remarked that, in principle, the least-squares method does not need a distribution model. The normality assumption may be employed, but it is not required. In contrast, both the LCD-based method and Bayesian approach require a distribution model. For the problem considered, both employ the normal distribution in the form of $N(\mu, \sigma_j^2)$ based on the fixed-effects model that does not account for the heterogeneity between the prior sample and the current sample. Therefore, the standard deviation of the posterior distribution obtained from either of the methods is essentially a conditional SU. The heterogeneity may be accounted for by employing a normal distribution in the form of $N(\mu, \tau^2 + \sigma_j^2)$ based on the random-effects model, where τ^2 is the heterogeneity variance.

Recall that, for the problem considered when σ is unknown, we employ $\hat{\sigma}$, an estimator of σ, in both the LCD-based method and the least-squares method. We could simply use the sample standard deviation s as $\hat{\sigma}$. However, we recommend using an unbiased estimator of σ. That is, $\hat{\sigma} = s/c_4$ and $\text{E}(s/c_4) = \sigma$, where $c_4 = \sqrt{\frac{2}{n-1}}\,\Gamma\left(\frac{n}{2}\right)/\Gamma\left(\frac{n-1}{2}\right)$, $\Gamma(.)$ stands for Gamma function. The unbiased estimator $\hat{\sigma}$ is recommended for uncertainty-based measurement quality control (Huang 2014); it is also adopted in the Type A uncertainty estimation (Huang 2018b) and in the unified theory of measurement errors and uncertainties (Huang 2018d). The approximate sampling distribution with $\hat{\sigma}$ as the scale parameter, i.e. Eq. (8), is recommended to replace the scaled and shifted t-distribution in Monte

Carlo simulation (Huang 2019b). Roesslein et al. (2007) also recommended using the unbiased estimator $\hat{\sigma}$ to avoid a significant underestimation of measurement uncertainty when the sample size is very small. The factor c_4 depends on the sample size n. It is 0.7979 for $n = 2$, 0.9400 for $n = 5$, and 0.9727 for $n = 10$. Therefore, the bias correction is only significant for small samples; it may be neglected when the sample size is greater than 10.

4. The Proposed Test for the Validity of a Prior

In practice, the availability of prior information does not mean one must incorporate the prior information into current measurement. The central to the combination is that the prior information is valid. The validity means that the prior information is representative of the current measurement. For example, measurement conditions have not changed over time so that the prior sample and the current sample are drawn from the same parent distribution. Phillips et al. (1998) presented an analysis example using the Bayesian approach for a production process. They pointed out that if the prior distribution is not representative of the current production process, the Bayesian adjustment would be inappropriate. However, Phillips et al. (1998) did not discuss about how to test for the validity of a prior.

The quality of the current sample mean $\bar{x}$ is measured by $\hat{\sigma}/\sqrt{n}$ (or $\sigma/\sqrt{n}$). The quality of $\hat{\mu}$ is measured by $\widehat{SU}_{conditional}$ or $\widehat{SU}_{unconditional}$, whichever is greater. Note that $\widehat{SU}_{conditional}$ is always smaller than $\hat{\sigma}/\sqrt{n}$, but $\widehat{SU}_{unconditional}$ could be greater than $\hat{\sigma}/\sqrt{n}$ if the squared residual $(x_{prior} - \hat{\mu})^2$ or $(\bar{x} - \hat{\mu})^2$ is very large. Intuitively, it does not make sense to combine the prior information with the current measurement if the SU of $\hat{\mu}$ is greater than the SU of $\bar{x}$. Thus, if $\widehat{SU}_{unconditional}$ is greater than $\hat{\sigma}/\sqrt{n}$, the prior information may be considered invalid and should not be incorporated into the current measurement.

We therefore propose a simple test for the validity of a prior. The ratio between $\widehat{SU}_{unconditional}$ and $\hat{\sigma}/\sqrt{n}$, denoted by SUR (standard uncertainty ratio), is taken as the test statistic

$$\mathrm{SUR} = \frac{\widehat{SU}_{unconditional}}{\hat{\sigma}/\sqrt{n}} \tag{17}$$

- If SUR ≤ 1, the prior is valid; take $\hat{\mu}$ as the estimate of the measurand. The SU of $\hat{\mu}$ is $\widehat{SU}_{conditional}$ or $\widehat{SU}_{unconditional}$, whichever is greater.
- If SUR > 1, the prior is invalid; do not combine the prior information with the current measurement. Instead, take the sample mean $\bar{x}$ as the estimate of the measurand. The SU of $\bar{x}$ is $\hat{\sigma}/\sqrt{n}$.

5. Examples

5.1 Example 1: Isotopic Ratio of Silver

Possolo and Bodnar (2018) conducted a Bayesian analysis of the measurement of the isotopic ratio R($^{107}Ag/^{109}Ag$) in commercial silver nitrate. The observation equation expresses each determination of the isotopic ratio as $R_j = \rho + \varepsilon_j$, for $j = 1, ..., n$, where ρ denotes the true value of the measurand, and the $\{\varepsilon_j\}$ denote (non-observable) measurement errors. Shields et al. (1960) made measurements and reported $r = 1.07547$ and $u(r)$=0.00065. Possolo and Bodnar (2018) assumed that the likelihood function, which is a function of ρ, is a Gaussian PDF with unknown mean ρ and known standard deviation $u(r)$=0.00065. They assigned to ρ a Gaussian prior distribution with mean 1.005 and standard deviation 0.003, based on the generally accepted value for ρ and uncertainty reported by Shields et al. (1960). The resulting posterior distribution is also normal with $\hat{\rho}_{SB} = 1.07231$ and SU_{SB} = 0.00064.

We applied the proposed LCD-based method and the least-squares method to this example. We assume that the prior distribution is normal with mean 1.005 and standard deviation 0.003; the current distribution is also normal with mean 1.07547 and standard deviation 0.00065. The proposed LCD-based method gives the same results as the Bayesian approach, i.e. $\hat{\rho} = \hat{\rho}_{SB} = 1.07231$ and $\widehat{SU} = SU_{SB} = 0.00064$. The least-squares method gives $\hat{\rho} = \hat{\rho}_{SB}$ = 1.07231, $\widehat{SU}_{conditional} = \widehat{SU} = SU_{SB} = 0.00064$, and $\widehat{SU}_{unconditional}$ = 0.01823.

Since SUR = 28, significantly greater than unity, according to the proposed test, the prior information is invalid and should not be combined with the current measurement. Thus, we should ignore the prior information and report r = 1.07547 and $u(r)$ = 0.00065 based on the current measurement only. If the prior information were combined with the current measurement, the weighted mean 1.07231 would have a much larger uncertainty ($\widehat{SU}_{unconditional}$ = 0.01823) than the sample mean of the current measurement.

5.2 Example 2: Voltage

Attivissimo et al. (2012) conducted a Bayesian analysis of the measurement of a voltage (V) with a Gaussian noise. The measurement gives a sample mean $\bar{V}$ = 2.5 mV. They assumed that the prior is a uniform distribution within the interval [-0.5, 5.5] mV, and the likelihood is a Gaussian PDF with unknown mean V and known standard deviation $\sigma = 1$ mV. Applying the Bayes rule, Attivissimo et al. (2012) gave an approximate posterior distribution that is normal with mean $\hat{V}_{SB}$ = 2.5 mV and standard deviation SU_{SB} = 1 mV.

We applied the proposed LCD-based method and the least-squares method to this example. We assume that

Method	$\widehat{V}$ (mV)	$\widehat{\mathrm{SU}}$ (mV)
LCD-based	2.5	1.0
Least-squares	2.5	0.866 (conditional) 0.0 (unconditional)
Bayesian (Attivissimo et al. 2012)	2.5	1.0

Table 1. Results for the measurement of voltage

the prior distribution is a uniform distribution within the interval [-0.5, 5.5] mV; the current distribution is normal with mean $\overline{V}$ = 2.5 mV and standard deviation σ = 1 mV. The LCD-based method was implemented with the one-dimensional PDS using an Excel spreadsheet. In the one-dimensional PDS, the range between -5 and 15 mV is divided into 200 intervals. Results for $\widehat{V}$ and $\widehat{\mathrm{SU}}$ are shown in Table 1.

Since $\widehat{\mathrm{SU}}_{\text{unconditional}}$ = 0, SUR = 0. According to the proposed test, the prior information is valid and should be combined with the current measurement. However, the prior is a uniform distribution over a large range; it is essentially a flat prior. A flat prior has no contribution to the posterior. Therefore, the posterior distribution is the same as the current distribution in the LCD-based method or the same as the normalized likelihood in the Bayesian approach.

Note that the least-squares method gives the same posterior mean as the LCD-based method. However, $\widehat{\mathrm{SU}}_{\text{conditional}}$ = 0.866 is different from $\widehat{\mathrm{SU}} = \mathrm{SU}_{\mathrm{SB}} = 1$. This is because, in this example, the prior is a uniform distribution. Consequently, the least-squares method does not give the "exact" solution as the LCD-based method or the Bayesian approach.

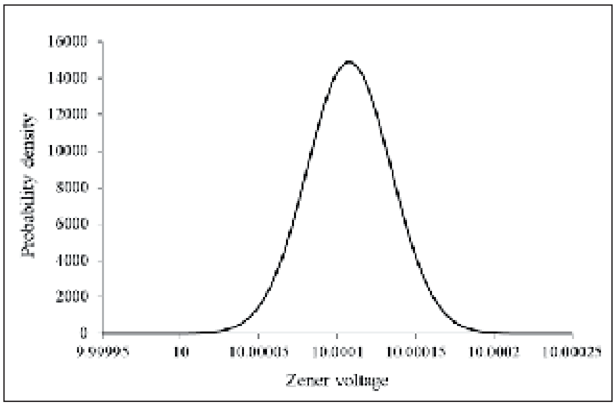

Figure 1. The combined PDF obtained with the one-dimensional PDS for the Zener voltage standard

5.3 Example 3: Zener Voltage Standard

Possolo and Bodnar (2018) conducted a Bayesian analysis for the example H.5 in the GUM (JCGM 2008) regarding the calibration of a Zener voltage standard that comprised five replicated determinations of a potential-difference made on each of 10 different days. The daily averages and experimental standard deviations are reported in table H.9 of the GUM. In their analysis, Possolo and Bodnar (2018) employed the random-effects model for the daily average $V_j = V + \lambda_j + \varepsilon_j$, for day $j = 1, \ldots, n$, where n = 10, denotes the number of days, the $\{\lambda_j\}$ denote day effects, and the $\{\varepsilon_j\}$ denote measurement errors. They treated the $\{\lambda_j\}$ as a sample from a Gaussian distribution with mean 0 and standard deviation τ, and the $\{\varepsilon_j\}$ as independent Gaussian random variables with mean 0 but different standard deviations $\{\sigma_j\}$. The prior distribution for V is Gaussian with mean 0 and a large standard deviation (a weak prior), and the prior distributions for τ and the {σj} are half-Cauchy. This is a 12-dimensional Bayesian problem because it has 12 unknown parameters: V, τ, and ten $\{\sigma_j\}$. The Bayesian hierarchical model was implemented in the NIST Consensus Builder (Koepke et al. 2017) with the application of MCMC sampling. Possolo and Bodnar (2018) also applied their Laplace approximation to this example. Van der Veen (2018) conducted a similar Bayesian analysis for this example.

We applied the LCD, Eq. (B.3), and the inverse-σ^2 WA (i.e. least-squares method) to this example. We assume that a daily sampling distribution is normal, $\widetilde{V}_j \sim N[\overline{V}_j,$

Method	$\widehat{V}$ (V)	$\widehat{\mathrm{SU}}$ (μV)
LCD: Eq. (B.3) (without c_4)	10.000108	25
LCD: Eq. (B.3) (with c_4)	10.000108	27
Inverse-σ^2 WA (without c_4)	10.000108	25
Inverse-σ^2 WA (with c_4)	10.000108	27
Bayesian (Possolo and Bodnar 2018)	10.000102	20
Bayesian (van der Veen 2018)	10.000103	21
Laplace approximation (Possolo and Bodnar 2018)	10.000097	12
GUM ANOVA (JCGM 2008)	10.000097	13 [GUM Eq. (H.28b)] 18 [GUM Eq. (H.32)]

Table 2. Results for the measurement of Zener voltage standard

$(\hat{\tau}^2 + \hat{\sigma}_j^2)]$, based on the random-effects model. However, the heterogeneity variance τ^2 (i.e. the between-day variance) estimated with the DerSimonian–Laird method (DerSimonian and Laird 1986) is negative so it is truncated to zero. Thus, the daily sampling distribution model reduces to $\widetilde{V}_j \sim \mathrm{N}(\overline{V}_j, \hat{\sigma}_j^2)$. The $\{\hat{\sigma}_j\}$ is estimated using the unbiased estimator $\hat{\sigma}_j = s_j / c_4$, where $c_4 = 0.94$ for five observations. For comparison, the biased estimator $\hat{\sigma}_j = s_j$ is also used in the analysis. The SU of the inverse-σ^2 WA is calculated as $\widehat{\mathrm{SU}} = 1/\sqrt{\Sigma_{j=1}^{n}(1/\hat{\sigma}_j^2)}$, which is the conditional SU (Huang 2019a). Since there is no prior information, there is no need to assume any prior distribution in applying the LCD, Eq. (B.3).

The LCD, Eq. (B.3), was implemented with the one-dimensional PDS using an Excel spreadsheet. In the one-dimensional PDS, the range between 0.998 and 10.002 V is divided into 2000 intervals. Figure 1 shows the combined PDF obtained from the one-dimensional PDS. Table 2 shows the results for $\widehat{V}$ and $\widehat{\mathrm{SU}}$. The GUM's ANOVA results, the Bayesian results of Possolo and Bodnar (2018) and van der Veen (2018), and the Laplace approximation of Possolo and Bodnar (2018) are also shown in Table 2 for comparison.

As expected, the LCD and the inverse-σ^2 WA give the same results because of the assumption of normality. Note that the bias correction using c_4 has no effect on $\widehat{V}$, but it results in a slight increase in $\widehat{\mathrm{SU}}$. The results of the LCD and the inverse-σ^2 WA are comparable with those of the Bayesian approach of Possolo and Bodnar (2018) and van der Veen (2018). However, the LCD with the one-dimensional PDS is much simpler than the Bayesian hierarchical model with the MCMC sampling.

It is important to note that, in this example the estimated SUs with the LCD and the inverse-σ^2 WA are the conditional SUs because the heterogeneity between days is negligible. We also estimated the unconditional SUs with Eq. (15). The results are 18 and 17 µV, with and without c_4 respectively, which are significantly smaller than the conditional SUs 25 and 27 µV, respectively. The discussion on the conditional and unconditional SUs in subsection 3.1 also applies to the inverse-σ^2 WA of multiple samples. Thus, the estimated "true" SU of the inverse-σ^2 WA should be the conditional SU or the unconditional SU, whichever is greater.

5.4 Example 4: Newtonian Constant of Gravitation

Koepke et al. (2017) conducted a Bayesian analysis of the Newtonian constant of gravitation G for a dataset that consists of the measurements from 14 laboratories (Mohr et al. 2012). Each laboratory reported their estimate G_j and the associated standard deviation σ_j (remark: the unit for G and σ is $/10^{-11}\mathrm{m}^3\mathrm{kg}^{-1}\mathrm{s}^{-2}$ that is omitted for simplicity). The dataset is shown in the Table 1 of Koepke et al. (2017).

In this study, we applied the LCD, Eq. (B.3), to this dataset. We assume that the sampling distribution at each laboratory is normal, $\widetilde{G}_j \sim N\,[G_j, (\hat{\tau}^2 + \sigma_j^2)]$, based on the random-effects model. The heterogeneity variance τ^2 (i.e. the between-laboratory variance) estimated with the DerSimonian–Laird method is $(0.00095)^2$. For comparison, we also assume that the sampling distribution at each laboratory is $\widetilde{G}_j \sim N\,(G_j, \sigma_j^2)$, based on the fixed-effects model. Again, since there is no prior information, there is no need to assume any prior distribution in applying the LCD, Eq. (B.3).

The LCD was implemented with the one-dimensional PDS using an Excel spreadsheet. In the one-dimensional PDS, the range between 6.64 and 6.74 is divided into 500

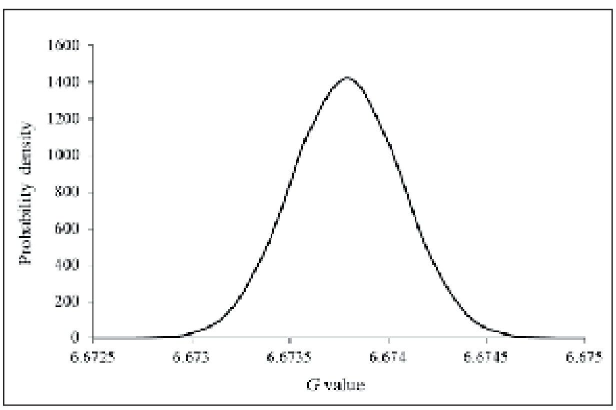

Figure 2. The combined PDF obtained with the one-dimensional PDS based on the random-effects model for the Newtonian constant of gravitation

Method		(unconditional)	(conditional)
LCD: Eq. (B.3) (based on the fixed-effects model)	6.67402	--	0.00006
LCD: Eq. (B.3) (based on the random-effects model)	6.67379	0.00028	--
Bayesian (Koepke et al. 2017)	6.67377	0.00033	--
DerSimonian–Laird (Koepke et al. 2017)	6.67380	0.00028	--
Inverse-σ2 WA (Huang 2019a)	6.67408	0.00025	0.00005
REML (Huang 2019a)	6.67390	0.00041	0.00013
DerSimonian–Laird (Huang 2019a)	6.67378	0.00031	0.00010

Table 3. Results for the measurement of Newtonian constant of gravitation

intervals. Figure 2 shows the combined PDF obtained with the one-dimensional PDS based on the random-effects model. Table 3 shows the results for $\widehat{G}$ and $\widehat{SU}$.

In addition, Koepke et al. (2017) applied the DerSimonian–Laird method to this example. Huang (2019a) applied the inverse-σ^2 WA, restricted maximum likelihood (REML) method, and DerSimonian–Laird method to this example. Their results are also shown in Table 3 for comparison.

It can be seen from Table 3 that the estimated G with all seven methods are consistent. The conditional $\widehat{SU}$ are significantly smaller than the unconditional $\widehat{SU}$. This is because there is significant heterogeneity between the laboratories (the estimated heterogeneity index I^2, also known as signal content index (SCI), is 0.76 (Huang 2019d)). As expected, the $\widehat{SU}$ estimated with the LCD based on the fixed-effects model is consistent with the conditional $\widehat{SU}$; the $\widehat{SU}$ estimated with the LCD based on the random-effects model is consistent with the unconditional $\widehat{SU}$. Moreover, all methods give comparable unconditional $\widehat{SU}$ (or $\widehat{SU}$ estimated with the random-effects model) except the REML method that gives a significantly high $\widehat{SU}$.

Discussion

6.1 Difference Between the LCD-based Method and the Bayesian Approach

There are several philosophical and methodological differences between the proposed LCD-based method and the Bayesian approach. First, in the proposed LCD-based method, the unknown parameter μ is treated as a fixed constant. This treatment complies with the concept of true values that is an important concept in measurement science. In contrast, in the Bayesian approach, the unknown parameter μ is treated as a random quantity ($\widetilde{\mu}$). This treatment may be acceptable in social sciences because in which there is essentially no objective truth. In measurement science, however, we assume that there exists the true value of a physical quantity, e.g. the location parameter μ in a distribution model (e.g. Huang 2018d). Because of the way statistics is still taught in most schools, for many practitioners the idea that the true value μ is a random quantity may be difficult to accept.

Second, the LCD-based method always deals with two distributions for the same quantity x. It gives one, and only one, posterior distribution of x. This logic framework is easy to understand, and the calculation is simple and straightforward because the problem is one-dimensional. For example, for the problem considered when σ is unknown, both the unknown parameters μ and σ in the current distribution model are estimated with point estimation. Consequently, the resulting posterior distribution of x is only a slight modification of the posterior distribution when σ is known. In contrast, in a Bayesian analysis, a prior distribution must be specified for each unknown parameter. A point estimation of unknown parameters is not allowed by Bayesians (otherwise it is not considered as Bayesian). For the problem considered when σ is unknown, the Bayesian approach has to employ a normal-Gamma prior to account for both the unknown parameters μ and σ (Murphy 2007). However, the Bayesian approach with the normal-Gamma prior is unable to provide a solution to the problem considered (refer to Appendix A). Moreover, a Bayesian approach supposes to give a posterior distribution for each unknown parameter. When multiple unknown parameters are involved in a problem, the Bayesian procedure may become very complicated.

Third, in the proposed LCD-based method, the prior and the current can be fully swapped. This is because both prior information and current information are represented by independent distributions. In fact, we could view a prior as the current and a current as the prior if we reverse time's arrow; the numerical results will be the same. In contrast, in the Bayesian setting, the prior and the current cannot be swapped. This is because prior information is represented by a probability distribution, whereas current information is represented by a likelihood function. The mathematical meaning of a probability distribution is not the same as that of a likelihood function. Fisher (1921) stated, "… probability and likelihood are quantities of an entirely different nature."

Fourth, the proposed LCD-based method is to be used only when prior information is available and current measurement is made. If prior information is available, but a measurement is not made, we solely rely on the prior information. If a measurement with multiple observations is made, but there is no prior information, we solely rely on the current measurement. It is important to note that frequentists are not forced to use a prior if there is no prior information. In contrast, Bayesians are forced to use a prior even if there is no prior information at all. They rely on "noninformative" priors such as the Jeffreys priors. However, the validity of the Jeffreys priors has been a subject of intense debate among Bayesians. For example, D'Agostini (1998), a leading proponent of Bayesian methods in particle physics, argued that "…it is rarely the case that in physical situations the status of prior knowledge is equivalent to that expressed by the Jeffreys priors, …" He further stated, "The default use of Jeffreys priors is clearly unjustified, especially in inferring the parameters of the normal distribution, …." Moreover, it is well known that the use of the Jeffreys priors with multiple observations leads to the t-distribution and t-interval. However, the use of the t-interval in measurement uncertainty analysis has been challenged in recent years. The author (Huang 2018a, 2018b) revealed that the t-based inference is invalid because of the "t-transformation distortion" and the t-interval is actually misused in uncertainty estimation.

Fifth, the proposed LCD-based method is easy to use.

The discrete form of the LCD, Eq. (2) or (B.3), is a one-dimensional PDS, which can be easily implemented with an Excel spreadsheet. In contrast, Bayesian approaches are not easy to implement, especially for high dimensional problems. Markov Chain Monte Carlo (MCMC) sampling was invented and can be used with great generality to produce samples from Bayesian posterior distributions (Robert and Casella 2011). However, the MCMC method requires considerable familiarity with specialized tools for statistical computing (Possolo 2015, Possolo and Bodnar 2018). The computational difficulties and lack of transparency associated with the Bayesian approach have been blamed for excessive effort being spent on understanding the computation and less effort being spent on model validation (Willink and White 2011).

6.2 More on Bayesian and Frequentist Methods with Respect to the Four Examples

Among the four examples, the first two examples have demonstrated the effectiveness of the proposed LCD-based method and the least-squares method for combining prior information with current measurement. The third and fourth examples have demonstrated the effectiveness of the LCD with the one-dimensional PDS for combining multiple distributions. The presented four examples indicate that the proposed frequentist methods produce equally good or better results with less complicated formulation and less computational effort than their Bayesian counterparts.

Note again that, in the third and fourth examples, there are no priors at all. So, our analyses using the LCD method are solely based on the measurement data (Type A information). In contrast, the noninformative priors or weak priors were assumed in the Bayesian methods of van der Veen (2018) and Possolo and Bodnar (2018). Because these priors are not real priors, they are expected to have little (or no) effects on the posterior distributions. However, if so, why bother using the assumed priors. Thus, it seems that, for these two examples, the assumed priors are redundant, and the use of the redundant priors do not offer any better inference than their frequentist counterparts that do not use any redundant prior. The use of the redundant priors seems just to make the Bayes theorem applicable, which actually leads to complicated formulation and calculation.

It is interesting to note that some proponents of Bayesian methods also appreciate the easiness of frequentist methods. Van der Veen (2018) proposed Bayesian methods for four Type A evaluations of SU and compared with classical frequentist methods. He commented that, in most real-world situations, Bayesian computations are much more involved (e.g. MCMC) than their frequentist counterparts. His examples showed "how classical statistical methods can be benchmarked against fully Bayesian ones." And he suggested, "if the differences are deemed to be meaningless, the simpler methods can be used in routine work."

7. Conclusion

This paper has demonstrated that frequentist statistics can provide simple and practical methods for combining prior information with current measurement in uncertainty analysis. It is a misperception that the combination can be made only with the Bayesian framework.

We emphasize that prior information must be valid. Combining invalid prior information with current measurement would deteriorate the quality of the estimation of the measurand. The proposed simple test can be used to determine whether a prior is valid. If a prior is invalid, it should not be incorporated into current measurement.

The law of combination of distributions (LCD) can be interpreted with Shannon's information theory. This leads to an information-theoretic formula, i.e. the "law of aggregation of information" (LAI), which offers new insight into the measurement process and uncertainty analysis. The LCD or LAI combines all available information to give aggregated information and improved inferences. In practice, the LCD can be easily implemented with the one-dimensional "probability domain simulation" using an Excel spreadsheet.

In general, Bayesian formulations are much more complicated, and Bayesian computations are much more involved (such as the MCMC sampling) than their frequentist counterparts. The frequentist methods (e.g. LCD, least-squares, and point estimation) can produce equally good or better results with less complicated formulation and less computational efforts than their Bayesian counterparts. Additionally, the use of redundant priors in Bayesian methods does not offer any better inference than their frequentist counterparts that do not use any redundant prior.

References

Attivissimo F, Giaquinto N, and Savino M. 2012. A Bayesian paradox and its impact on the GUM approach to uncertainty. *Measurement* 45 2194–2202. DOI:10.1016/j.measurement.2012.01.022

Clemen R T and Winkler R L. 1999. Combining probability distributions from experts in risk analysis. *Risk Analysis* 19 187-203.

D'Agostini G. 1998. Jeffreys priors versus experienced physicist priors: arguments against objective Bayesian theory. *Proceedings of the 6th Valencia International Meeting on Bayesian Statistics* (Alcossebre, Spain, May 30th-June 4th).

DerSimonian R and Laird N. 1986. Meta-analysis in clinical trials. *Controlled Clinical Trials* 7 177–188.

Fisher R A. 1921. On the 'Probable Error' of a coefficient of correlation deduced from a small sample. *Metron* I: 3-32.

Gelman A, Carlin J B, Stern H S, Dunson D B, Vehtari A, and Rubin D B. 2014. *Bayesian Data Analysis* 3rd edition, CRC Press, (ISBN 978-1-4398-4095-5).

Huang H. 2014. Uncertainty-based measurement quality control. *Accreditation and Quality Assurance* 19 65-73.

Huang H. 2018a. Uncertainty estimation with a small number of measurements, Part I: new insights on the t-interval method and its limitations. *Measurement Science and Technology* 29. https://doi.org/10.1088/1361-6501/aa96c7

Huang H 2018b. Uncertainty estimation with a small number of measurements, Part II: a redefinition of uncertainty and an estimator method. *Measurement Science and Technology* 29. https://doi.org/10.1088/1361-6501/aa96d8

Huang H. 2018c. A new method for estimating consensus value in interlaboratory comparison. *Metrologia* 55 106-113. https://doi.org/10.1088/1681-7575/aaa170

Huang H. 2018d. A unified theory of measurement errors and uncertainties. *Measurement Science and Technology* 29 125003. https://doi.org/10.1088/1361-6501/aae50f

Huang H 2019a. A unified formula for uncertainty estimation in interlaboratory studies and key comparisons. *CAL LAB: the International Journal of Metrology* 26(4): 22-29.

Huang H. 2019b. Why the scaled and shifted t-distribution should not be used in the Monte Carlo method for estimating measurement uncertainty? *Measurement* 136 282-288. https://doi.org/10.1016/j.measurement.2018.12.089

Huang H 2019c. On the Bayesian estimator of normal mean, discussion at *ResearchGate* https://www.researchgate.net/post/On_the_Bayesian_estimator_of_normal_mean

Huang H 2019d. Signal content index (SCI): a measure of the effectiveness of measurements and an alternative to *p*-value for comparing two means. *Measurement Science and Technology*. https://doi.org/10.1088/1361-6501/ab46fd

Huang H 2020. Comparison of three approaches for computing measurement uncertainties. *Measurement* 163. DOI: 10.1016/j.measurement.2020.107923

Huang H and Fergen R E. 1995. Probability-domain simulation - A new probabilistic method for water quality modeling. *WEF Specialty Conference* "Toxic Substances in Water Environments: Assessment and Control" (Cincinnati, Ohio, May 14-17, 1995).

Joint Committee for Guides in Metrology (JCGM). 2008. *Evaluation of measurement data - Guide to the expression of uncertainty in measurement* (GUM 1995 with minor corrections), Sevres, France.

Koepke A, Lafarge T, Possolo A and Toman B. 2017. Consensus building for interlaboratory studies, key comparisons, and meta-analysis. *Metrologia* 54 S34–S62.

Landauer R. 1961. Irreversibility and heat generation in the computing process. *IBM Journal of Research and Development* 5 183-191.

Merkatas C, Toman B, Possolo A, Schlamminger S. 2019. Shades of dark uncertainty and consensus value for the Newtonian constant of gravitation. *Metrologia* DOI: 10.1088/1681-7575/ab3365

Mohr PJ and Taylor B N. 2000. CODATA recommended values of the fundamental physical constants:1998 *Reviews of Modern Physics* 72 351–495. doi: 10.1103/RevModPhys.72.351

Mohr P J, Taylor B N, and Newell D B. 2012. CODATA recommended values of the fundamental physical constants: 2010 *Rev. Mod. Phys.* 84 1527–605.

Murphy K P. 2007. Conjugate Bayesian analysis of the Gaussian distribution. Last updated Oct 3, 2007, https://www.cs.ubc.ca/~murphyk/Papers/bayesGauss.pdf

Phillips S D, Estler W T, Levenson M S and Eberhardt K R. 1998. Calculation of measurement uncertainty using prior information. *J. of Research of the National Institute of Standard and Technology* 103 625-32.

Possolo A. 2015. *Simple Guide for Evaluating and Expressing the Uncertainty of NIST Measurement Results* NIST Technical Note 1900, National Institute of Standards and Technology. DOI:10.6028/NIST.TN.1900

Possolo A and Bodnar O. 2018. Approximate Bayesian evaluations of measurement uncertainty. *Metrologia* 55 147–157. https://doi.org/10.1088/1681-7575/aaa5be

Robert C and Casella G. 2011. A short history of Markov Chain Monte Carlo: subjective recollections from incomplete data. *Stat. Sci.* 26 102–15

Roesslein M, Wolf M, and Wampfler B. 2007. A forgotten fact about the standard deviation *Accreditation and Quality Assurance* 12 495. https://doi.org/10.1007/s00769-007-0285-2

Rossi G B. 2014. *Measurement and Probability, A Probabilistic Theory of Measurement with Applications* Springer Netherlands pp286.

Shannon C E. 1948. A Mathematical Theory of Communications *The Bell System Technical Journal* 27 379-423, 623-656.

Shields W R, Craig D N and Dibeler V H. 1960. Absolute isotopic abundance ratio and the atomic weight of silver *J. Am. Chem. Soc.* 82 5033–6.

Sidik K and Jonkman J N. 2002. A simple confidence interval for meta-analysis *Statistics in Medicine* 21 3153-3159. DOI:10.1002/sim.1262

Van der Veen A M H. 2018. Bayesian methods for type A evaluation of standard uncertainty *Metrologia* 55 670–684. https://doi.org/10.1088/1681-7575/aad103

Wile J L. 2012. Information is a real, physical quantity *Proslogion*. https://blog.drwile.com/information-is-a-real-physical-quantity/

Willink R and White D R. 2011. *Disentangling classical and Bayesian approaches to uncertainty analysis*, Measurement Standards Laboratory, PO Box 31310, Lower Hutt 5040, New Zealand.

Hening Huang (heninghuang1@gmail.com), Teledyne RD Instruments, Retired.

Appendix A. Bayesian Solutions to the Problem Considered

Bayesians treat the unknown parameter μ as a random quantity that is denoted by $\tilde{\mu}$ here to distinguish it from μ. In the Bayesian setting, prior information is represented by a prior distribution of $\tilde{\mu}$ (simply called prior), denoted by $p_{\text{prior}}(\tilde{\mu})$. Current knowledge is represented by a likelihood function (simply called likelihood). The prior is combined with the likelihood through a reformulated Bayes Theorem to give a posterior distribution of $\tilde{\mu}$, denoted by $p_{\text{post}}(\tilde{\mu})$

$$p_{\text{post}}(\tilde{\mu}) \propto \text{likelihood}(\tilde{\mu}) \times p_{\text{prior}}(\tilde{\mu}) \quad \text{(A.1)}$$

For the problem considered when σ is known, the prior PDF of $\tilde{\mu}$ is normal with mean x_{prior} and variance σ^2_{prior}. That is

$$p_{\text{prior}}(\tilde{\mu}) = N(\tilde{\mu} \mid x_{\text{prior}}, \sigma^2_{\text{prior}}) \quad \text{(A.2)}$$

The likelihood function with n observations can be written as (Murphy 2007, p.2)

$$\text{likelihood}(\tilde{\mu}) \propto \exp\left(-\frac{n}{2\sigma^2}(\bar{x}-\tilde{\mu})^2\right) \propto N(\tilde{\mu} \mid \bar{x}, \frac{\sigma^2}{n}) \quad \text{(A.3)}$$

According to Eq. (A.1), the posterior PDF of $\tilde{\mu}$ can be written as

$$p_{\text{post}}(\tilde{\mu}) \propto N(\tilde{\mu} \mid \bar{x}, \frac{\sigma^2}{n}) \times N(\tilde{\mu} \mid x_{\text{prior}}, \sigma^2_{\text{prior}}) \quad \text{(A.4)}$$

Thus, $p_{\text{post}}(\tilde{\mu}) = N(\tilde{\mu} \mid x_{\text{post}}, \sigma^2_{\text{post}})$. The posterior mean x_{post} is taken as the estimate of μ (denoted by $\hat{\mu}_{\text{SB}}$) and the square root of the posterior variance σ^2_{post} is the SU (denoted by SU_{SB}) of $\hat{\mu}_{\text{SB}}$. That is

$$\hat{\mu}_{\text{SB}} = \frac{\frac{x_{\text{prior}}}{\sigma^2_{\text{prior}}} + \frac{\bar{x}}{\sigma^2/n}}{\frac{1}{\sigma^2_{\text{prior}}} + \frac{1}{\sigma^2/n}} \quad \text{(A.5)}$$

$$\text{SU}_{\text{SB}} = \frac{1}{\sqrt{\frac{1}{\sigma^2_{\text{prior}}} + \frac{1}{\sigma^2/n}}} \quad \text{(A.6)}$$

When σ is unknown, Bayesians treat σ as a random quantity that is denoted by $\tilde{\sigma}$ to distinguish it from σ. Thus, both $\tilde{\mu}$ and $\tilde{\sigma}$ are random quantities. Accordingly, the likelihood function with n observations becomes (Murphy 2007, p.6)

$$\text{likelihood}(\tilde{\mu}, \tilde{\lambda}) = \frac{1}{(2\pi)^{n/2}} \tilde{\lambda}^{n/2} \exp\left(-\frac{\tilde{\lambda}}{2}[n(\tilde{\mu}-\bar{x})^2 + \Sigma_{i=1}^{n}(x_i-\bar{x})^2]\right) \quad \text{(A.8)}$$

where $\tilde{\lambda} = 1/\tilde{\sigma}^2$.

Murphy (2007, p.6) assumed a normal-Gamma prior to account for the unknown parameters μ and σ

$$p_{\text{prior}}(\tilde{\mu}, \tilde{\lambda}) = \frac{1}{Z_{NG}} \tilde{\lambda}^{\alpha_0 - 1/2} \exp\left(-\frac{\tilde{\lambda}}{2}\left[\kappa_0(\tilde{\mu}-x_{\text{prior}})^2 + 2\beta_0\right]\right) \quad \text{(A.9)}$$

$$Z_{NG} = \frac{\Gamma(\alpha_0)}{\beta_0^{\alpha_0}}\left(\frac{2\pi}{\kappa_0}\right)^{1/2} \quad \text{(A.10)}$$

where $\Gamma(.)$ stands for Gamma function, κ_0 is the equivalent sample size of the prior, α_0 and β_0 are the shape parameter and rate parameter respectively for the Gamma distribution.

Murphy (2007) gives a posterior that is also normal-Gamma. However, his solution is not applicable to the problem considered in this paper because the values for κ_0, α_0, and β_0 are not available. Gelman et al. (2014) give a similar solution to that of Murphy (2007) using the normal-inverse χ^2 prior. Their solution requires the information on the degrees of freedom and scale of $\tilde{\sigma}^2$ that is not available for the problem considered either. Therefore, the Bayesian approach is unable to provide a solution to the problem when σ is unknown (without additional information). An extensive discussion titled "On the Bayesian estimator of normal mean" at ResearchGate has confirmed this situation (Huang 2019c).

Appendix B. The Law of Combination of Distributions (LCD)

Suppose we are considering N independent random variables X_j ($j = 1, 2, 3, \ldots N$), each of which has a probability density function (PDF) denoted by $p_j(x_j)$. We assume that all PDFs have the same support on the real line, i.e. $x_j \in (-\infty, +\infty)$. According to the product rule for independent random variables, the joint distribution of X_i can be written as

$$p(x_1, x_2, x_3 .. x_N) = \prod_{j=1}^{N} p_j(x_j) \quad \text{(B.1)}$$

Equation (B.1) represents a multivariate distribution of N independent random variables.

We are interested in the probability distribution, denoted by $p_c(x)$, of the same outcome x drawn from the multivariate distribution, i.e. $x = x_1 = x_2 = x_3 \ldots = x_N$. Apparently, $p_c(x)$ is a single-variate distribution of x; it can be written as

$$p_c(x) = \frac{\prod_{j=1}^{N} p_j(x)}{\int \prod_{j=1}^{N} p_j(x)dx} \quad \text{(B.2)}$$

where $\int \prod_{j=1}^{N} p_j(x)dx$ is the scale factor that ensures the integration of $p_c(x)$ is one.

Equation B.2 is essentially identical to a formula given in Rossi, (2014, p.230), but without defining the scale factor, nor providing a demonstration.

An analytical solution to $p_c(x)$ may be available for some problems. For example, if all $p_j(x)$ are Gaussian PDFs, $p_c(x)$ is also a Gaussian PDF. When an analytical solution to Eq. (B.2) is not available, a numerical solution to $p_c(x)$ can be obtained using a discretized form of Eq. (B.2)

$$p_c(x_i) = \prod_{j=1}^{N} p_j(x_i) / \Sigma_{i=1}^{m} \prod_{j=1}^{N} p_j(x_i) \qquad \text{(B.3)}$$

in which, the range of x that supports $p_j(x)$ is divided into m intervals. In fact, Eq. (B.3) is a one-dimensional "probability domain simulation" (PDS), a probabilistic procedure (Huang and Fergen 1995). Detailed discussion on the PDS and comparison with its counterpart: "sampling-domain simulation", i.e. Monte Carlo simulation, can be found in Huang and Fergen (1995).

We designate Eq. (B.2) or Eq. (B.3) as the "law of combination of distributions" (LCD). Appendix C demonstrates the LCD. The essence of the LCD is the way of using PDFs, regardless of whether a PDF is based on the frequentist view of probability or based on the Bayesian view of degree of belief.

The LCD can be interpreted with Shannon's information theory. The information content of an outcome $\{x\}$ that is drawn from the distribution $p_j(x)$ can be written as $I_j(x) = -\log[p_j(x)]$ (Shannon 1948). Thus, the LCD, Eq. (B.2), can be rewritten in terms of information content as

$$I_c(x) = \Sigma_{j=1}^{N} I_j(x) - I_0 \qquad \text{(B.4)}$$

where $I_c(x)$ is the aggregated information and I_0 is written as

$$I_0 = -\log\left[\Sigma_{i=1}^{m} \prod_{j=1}^{N} p_j(x_i)\right] \qquad \text{(B.5)}$$

I_0 is always positive because the scale factor is always less than unity. Therefore, Eq, (B.4) suggests that the information content of x_i decreases, i.e. the uncertainty about x_i decreases, after the aggregation of the information from multiple sources.

We designate Eq. (B.4) as the "law of aggregation of information" (LAI). Landauer (1961) argued that information is a real, physical quantity that is governed by the second law of thermodynamics (Wile 2012). Clemen and Winkler (1999) also view information as a physical magnitude. In the light of this, the LAI could be of use also in problems of physics.

Appendix C. Demonstration of the LCD

Let us consider two independent random variables X and Y that have different discrete distributions with the same support. We assume that there are three events in X and Y, X:$\{x_1, x_2, x_3\}$=$\{0, 1, 2\}$ and Y:$\{y_1, y_2, y_3\}$=$\{0, 1, 2\}$, with the probabilities P_x:{0.2, 0.3, 0.5} and P_y:{0.3, 0.3, 0.4} respectively. All possible joint events of X and Y, $\{x_i \cap y_j\}$ (i, j=1, 2, and 3), are shown in Table C.1. The probabilities on

(0∩0)	(0∩1)	(0∩2)
(1∩0)	(1∩1)	(1∩2)
(2∩0)	(2∩1)	(2∩2)

Table C.1 Joint events of X and Y, $\{x_i \cap y_j\}$ (i, j =1, 2, and 3)

0.06	0.06	0.08
0.09	0.09	0.12
0.15	0.15	0.2

Table C.2 Probabilities on the joint events shown in Table 6, P_{ij} (i, j =1, 2, and 3)

the joint events, P_{ij} (i, j=1, 2, and 3), are shown in Table C.2.

The joint probability matrix (Table C.2) is a bivariate discrete distribution of X and Y. In the problem concerned, however, the object of interest is the chances of the "same events" happening simultaneously, i.e. (0∩0), (1∩1), and (2∩2). Note that these events are on the main diagonal of the joint event matrix (Table C.1), and the corresponding probabilities are on the main diagonal of the joint probability matrix (Table C.2): P_{11}, P_{22}, and P_{33}, which are known as the diagonal probabilities in statistics. The diagonal events and associated diagonal probabilities constitute a (unnormalized) single-variate discrete distribution of Z:{0, 1, 2}. After the normalization of the diagonal probabilities, the probabilities of Z:{0, 1, 2} are: P_z:{0.171, 0.257, 0.571}. Thus, the bivariate discrete distribution of X and Y collapses to the single-variate discrete distribution of Z. This logical operation can be readily extended to a multivariate discrete distribution; it is also applicable to continuous distributions.

It is important to note that there is the physics behind the logical operation described above. In fact, the logical operation mimics the physical process of receiving the messages from two independent sources (i.e. transmitters) X and Y by a receiver Z. The transmitters X and Y send messages that are coded as X:{0, 1, 2} and Y:{0, 1, 2}, with probabilities P_x:{0.2, 0.3, 0.5} and P_y:{0.3, 0.3, 0.4} respectively. The receiver Z is designed (e.g. with a filter) to only accept the same messages the transmitters X and Y send simultaneously, i.e. (0∩0), (1∩1), and (2∩2), ignoring other messages. Thus, the receiver Z outputs the coded messages Z:{0, 1, 2} with the probabilities P_z:{0.171, 0.257, 0.571}. This physical process can be nicely described with Shannon's information theory, leading to the "law of aggregation of information" (LAI), as discussed in Appendix B.

Sampling with a 3458A Type DMM

Rado Lapuh
Left Right d.o.o.

There is often a need in metrology to use a high precision sampling digital multi-meters in order to look at the amplitude, frequency and phase of a sinewave signal in detail. But sampling these signals and correctly configuring the meter is not always an easy task. Additionally, the meter's sampling configuration and data processing will affect the overall estimated measurement uncertainty of the signals being sampled. This paper will cover the complexities of sampling signals and their effects on the measurement uncertainties. It will also have some examples on the use and configuration of the Keysight 3458A with MATLAB examples for Sine Fitting and a Phase Sensitive Frequency Estimator returning amplitude, phase and offset of the signal.

Introduction

DMMs have since long time evolved from simple voltage-current-resistance measuring instruments into truly multifunction measurement devices. Apart from numerous functions, you can now use a DMM's front panel to set up repetitive measurements with complex triggers and graphically display histograms and trends of the captured data. This can work great for developers and engineers in need to quickly track down the behavior of their new electronic device or a production plant.

However, calibration labs need to rely on well understood, verified and documented procedures to perform calibrations, which can be repeated at any time. This often requires using software to capture data and remotely operate the DMM and a unit under test. Often, such software would simply program and collect DMM measurements on a desired function.

But, there are more complex problems in a calibration lab that require, additional to a dedicated measurement setup, to sample signals and use dedicated signal processing to arrive to a desired measurement result and an associated uncertainty. Examples would be measurement of electrical power, power quality parameters, phase, harmonic distortions, voltage or current ratios, to name a few. So, to utilize a DMM sampling in a calibration lab, a number of prerequisites should be considered, together with understanding detailed DMM capabilities, often requiring some of their parameters, which are even not included in their manufacturer specifications. Here, we will try to collect and explain them for most sampling scenarios using a Keysight 3458A type DMM.

What is Sampling?

Sampling a voltage signal is conceptually very simple: it requires taking N voltage measurements at times, equally separated by a sampling time t_s. With this process, the continuous-time signal is converted to its discrete-time representation. Both the analog to digital conversion and its timing plays a crucial role in final accuracy of the measurement. With ideal conversion and timing, no information of the continuous-time signal is lost, if this signal contains no spectral components above the half of sampling frequency. This information can be recovered by signal processing. When an integer number of signal periods is sampled with N samples, this can be achieved using FFT. In other cases, more complicated algorithms might be appropriate. The whole process is shown on Figure 1. While the sampling can be used to measure almost any signal parameter beyond the measurements built into a DMM, it typically requires writing dedicated software to capture and transfer data to a computer and perform adequate signal processing. However, when done correctly, it can provide for a measurement performance which is out of reach for any out-of-the-box instrument. That was proven and published with numerous examples in the NMIs worldwide, with a number of new articles appearing at this year's NCSLI/CPEM virtual conference.

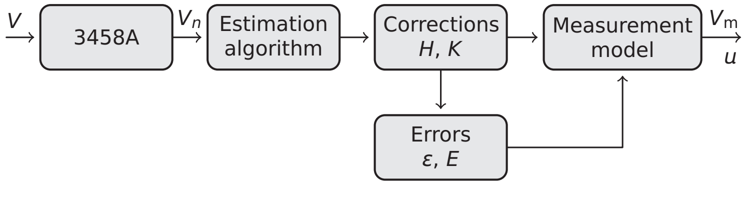

Figure 1. The principal process of obtaining measurement result from sampling the signal.

3458A Analog to Digital Converter

Integrating an analog-to-digital converter (IADC) converts the analog signal to its digital representation by integrating the signal amplitude over a predefined aperture time.

The 3458A achieves its performance with its custom built, multi-slope IADC and advanced triggering. This IADC was developed more than 30 years ago, being regarded as a major breakthrough at that time, and its performance is still on the state-of-the-art level even today. As all accurate DMMs use the IADC principle, it is not surprising to state that IADC is the most accurate analog-to-digital converter for low frequency signals. There are a few reasons for that. First, is its inherent property of increasing its resolution with increasing integration (aperture) time. Second, the aperture time provides for a low pass filter, which rejects any high frequency signals from interfering with the measurement. Third, this low pass filter characteristic is mathematically known to an unprecedented accuracy, allowing to almost perfectly compensate for its attenuation and delay effects.

Let us collect the most important DMM characteristics when used for sampling, providing a 3458A performance along as a benchmark [1]. Two of them, aperture time roll-off and input filter roll-off, can be compensated for to a certain degree. The rest of them, which are all of random nature, cannot be compensated and enter directly into the uncertainty budget.

Aperture Time Roll-Off

As already said, the IADC converts the input signal value by integrating the input signal over the aperture time t_a, as illustrated on Figure 2. The numerical value, obtained during this process, represents the average amplitude of the input signal during the integration

$$V_{\mathrm{IADC}} = \frac{1}{t_{\mathrm{a}}} \int_{t_{\mathrm{n}} - \mathrm{t_a}/2}^{t_{\mathrm{n}} + \mathrm{t_a}/2} V(t)\, \mathrm{d}t. \tag{1}$$

Due to the averaging process, this will act as a filter for the input signal, with a frequency response shown on Figure 3 and given by

$$H_{\mathrm{t_a}} = \frac{\sin(\pi\, f\, t_{\mathrm{a}})}{\pi\, f\, t_{\mathrm{a}}}. \tag{2}$$

Poles at positive integer multiples of $1/t_a$ provide a complete attenuation of the input signal. The bounding slope of this roll-off is defined as $20\log_{10}(\pi f t_a)$ and is equal to 20 dB per decade or 6 dB per octave. For the frequencies below $1/t_a$, it can be seen as the single pole filter with cut-off frequency of $0.443/t_a$.

Actually, the high frequency signals are attenuated more strongly than with a single pole filter. By carefully selecting the $1/t_a$, certain high frequency signals such as harmonic components can be almost completely filtered out during the sampling process. This is essential when sampling DC voltage, where the best choice is to select the aperture time as an integer multiple of line frequency period.

The 3458A aperture time can be programmed from 500 ns to 1 s in steps of 100 ns. The resulting attenuation, given by Eq. 2, is necessary to take into account separately for each spectral line measured in such a way, that the measured spectral line amplitude at frequency f is divided by $H_{\mathrm{t_a}}$ calculated for that frequency.

Despite the strong effect the aperture time might have on the sampled AC waveform amplitude, it can be corrected with a very high accuracy. To support this statement [2], using an aperture time of 1 ms when sampling a 100 Hz sine wave signal, the error of −16368 μV/V could be corrected using Eq. 2 with an uncertainty of less than 3 μV/V. Note, however, that additional errors will add up with shorter aperture times and there is a jump below 100 μs where a high-speed mode replaces the high-resolution

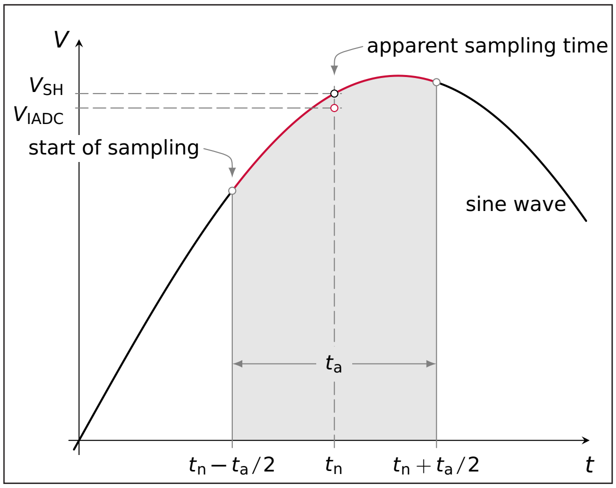

Figure 2. Interpretation of the integrating ADC conversion and its measured value V_{IADC}. The sample-hold driven (e.g. SAR) ADC would return V_{SH} if its sampling would start $t_a/2$ later.

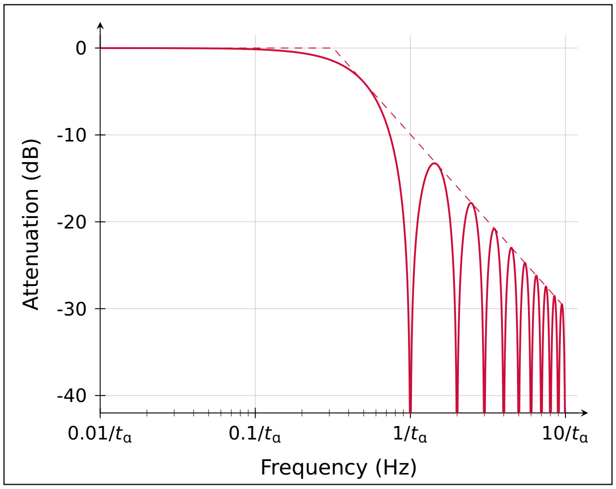

Figure 3. IADC inherent frequency response as a function of frequency.

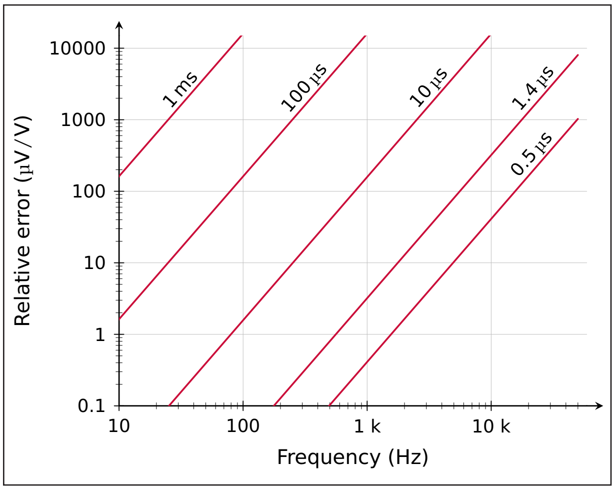

Figure 4. The IADC amplitude error for a few typical aperture times as a function of signal frequency.

mode. Nevertheless, the 3458A demonstrated exceptional accuracy in sampling mode better than ±20 µV/V at signal frequencies up to 3.3 kHz [3].

When it is necessary to correct for the aperture time roll-off, actually depends on the signal frequency being measured and the aperture time used for its measurement. Figure 4 plots selected aperture times and their effect as a function of signal frequency.

Input Filter Roll-Off

Before the signal is sampled, it is routed through the DMM input circuitry, which might attenuate or amplify the signal (none of these is applied on 10 V range), provide for over-range protection etc. Additionally, there is typically a simple RC input filter, which attenuates higher frequency signals to suppress high frequency interferences. The frequency response of this filter can be easily measured even with a modern arbitrary waveform generator, which is flat enough to measure the filter −3 dB attenuation frequency point. For the 3458A, input filter frequency response on all ranges is shown on Figure 5. Its −3 dB attenuation frequency points are approximately at 165 kHz and 120 kHz for 1 V and 10 V ranges, respectively.

The single pole model is sufficient to describe the 3458A's frequency response very accurately up to a few kHz frequency band for the 1 V and 10 V ranges using nominal values for −3 dB attenuation frequency point (f_{3dB}) [3], but can be used across the whole audio frequency band if this point is measured more accurately [4]

$$H_{1p} = \frac{1}{\sqrt{1+\left(\frac{f}{f_{3dB}}\right)^2}}. \tag{3}$$

The equalization of the input filter roll-off can be performed similarly as described for the aperture time roll-off, by dividing the measured spectral line amplitude at frequency f by H_{1p} calculated for that frequency.

For the µV/V accuracy measurements on 1 V and 10 V ranges, this input filter roll-off would affect the measured signal level that is already below 200 Hz or below 0.17 % of the DMM bandwidth. The input filter roll-off can be simply and still accurately equalized for frequencies up to 3.3 kHz [3] or up to 2.8 % of the DMM bandwidth.

DMM (Effective) Resolution

Here we briefly discuss the DMM term (effective) resolution and its possible confusion with typical ADC resolution specification. Typical ADC, be it successive approximation (SAR) or now popular Sigma-Delta (Σ-Δ) type, is commonly specified in number of bits, say 16 bits (for SAR) or 24 bits (for audio Σ-Δ). These specifications are their numerical resolutions, representing the ultimate resolution of the conversion in terms of a number of counts generated and thus the word length of the output digital format. For DMMs, as measuring devices, this is not a very useful specification; they are rather specified using an effective resolution, which also includes other imperfections like differential non-linearity and noise. As differential linearity error is typically very low for IADC (0.02 µV/V for 3458A), the effective resolution assumes less than one count of rms noise. The effective resolution as a function of the aperture time is an essential specification for a DMM. For 3458A, it is plotted on Figure 6 (on the next page), together with its numerical resolution.

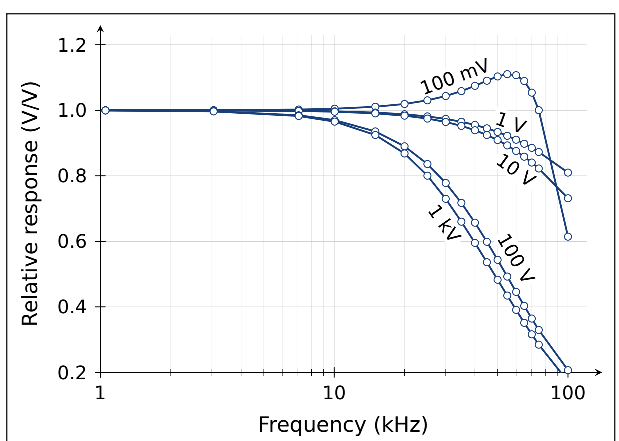

Figure 5. The measured 3458A's DCV mode input filter frequency response for all ranges.

Noise

The noise captured in the sampling process is always a combination of signal noise and digitizer noise. Digitizer noise is further a combination of input circuitry noise and a time jitter noise. The later increases with increasing signal frequency and amplitude and will be discussed separately. The input circuitry noise depends on the aperture time selected. It can be measured by short circuiting the input terminals and sampling a number of short bursts of residual noise voltages V_n at selected aperture times. The RMS noise value can be calculated from each burst by computing its standard deviation

$$\sigma_{\mathrm{n}} = \frac{1}{N-1}\sum_{n=0}^{N-1} V_n^2. \tag{4}$$

The resulting signal-to-noise ratio can be calculated against full scale signal at a given range using

$$SNR = 20 \cdot \log_{10}\left(\frac{\mathrm{Range}/\sqrt{2}}{\sigma_{\mathrm{n}}}\right). \tag{5}$$

Figure 7 plots measured 3458A SNR for 1 V and 10 V ranges. Red lines represent the 3458A effective resolution specification. Two things emerge instantly form these graphs. First is the already mentioned change-over from the high-speed mode to the high-resolution mode at 100 µs aperture time. Second is the inability of the 3458A to cope with its specification at aperture times above 100 ms or so. The reason for this behavior is in the 1/*f* noise, which starts to dominate at frequencies below a few Hz. The effect is more strongly pronounced on the 1 V range, as the input amplifier seems to add 1/*f* noise of its own to the final combined noise.

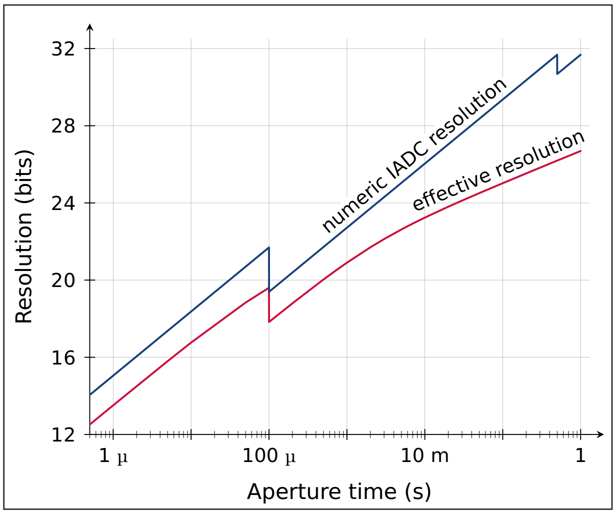

Figure 6. The 3458A's IADC (effective) resolution in bits for the DINT data format.

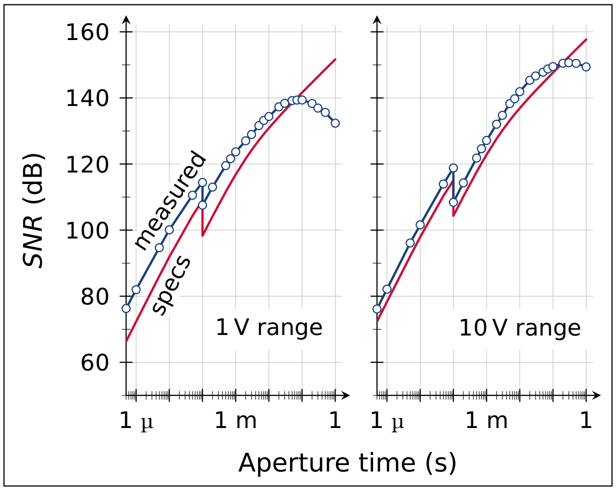

Figure 7. The 3458A's input stage and the IADC noise as measured using the short circuited input.

Time Jitter

Every clock governing a sampling process has a timing instability, known as a sample clock jitter. If the clock jitter is a random white noise process—and it usually is—the noise added to the perfect sine wave sampled is proportional to the sine wave frequency and the amplitude of the jitter noise. The jitter noise therefore limits the accuracy of a sampling system at higher signal frequencies.

The amplitude of the jitter noise strongly depends on the sampling time base source used, where the instrument's internal time base typically provides the lowest jitter noise.

This is definitely true for the 3458A, where the internal time jitter standard deviation is specified at 100 ps, but when using an external sampling clock source, it is specified at 50 ns, which is almost three orders of magnitude higher. When an external trigger clock source is used to trigger each sample performed by the 3458A, care should be taken not to introduce an additional error into the sampling process that is caused by trigger source timing jitter.

Since the use of an external trigger is almost unavoidable when synchronizing two 3458As, it is important to both understand the operation of the 3458A's timing circuitry and also to evaluate its time jitter performance.

In effect, the full scale sine wave sampled with the effective[1] time jitter t_{j} will result in the following signal to noise ratio

$$SNR = -20 \cdot \log_{10}\sqrt{\left(\frac{\sigma_{\mathrm{n}}}{V_{\mathrm{RMS}}}\right)^2 + \left(2\pi f\, t_j\right)^2}\,, \tag{6}$$

where V_{RMS} is sine wave RMS amplitude, *f* is sine wave frequency and σ_{n} is the white noise RMS voltage. From Eq. 6 we can see that the time jitter related noise (right part under the square root) is independent of DMM white noise and can,

1 Time jitter with normal (Gaussian) distribution.

if the time jitter is excessive and the signal frequency is high enough, completely hamper the DMM SNR performance.

For the 3458A, with its measured 145 ps time jitter noise, this is not the case when internal timer is used to dictate sampling. However, when using external trigger as a sampling clock source, the internal 3458A timing circuitry will build around 6 ns effective time jitter. For an idea of it, this jitter would limit the SNR for a full scale sine wave at 60 Hz to 113 dB and at 1000 Hz at 88 dB.

Other Timing Errors

Other timing errors might become important when two signals must be captured synchronously with two DMMs. A good example is a power measurement, where one DMM is sampling voltage signal and the other is sampling current signal. While two DMMs can be operated synchronously by providing a common trigger signal or in a master-slave fashion, internal DMM delays would influence the resulting power calculation through the phase displacement, caused by such delays. In certain cases, such delays can be simply measured and compensated for by applying a common input signal at the frequency of interest and measuring the phase difference using a DMM's synchronization mode of choice.

Signal Analysis

Once the samples were acquired by the DMM or perhaps by a multiple of them, it is necessary to perform signal processing on them. As it was already pointed out in the previous sections, the sampled values do not represent the actual signal values, as they were modified by filtering effects of aperture time and input filter both in amplitude and in phase. However, these effects can be compensated with a very good accuracy. The magnitude of the filtering effect depends on signal frequency, so it is only natural to first extract individual frequency components from the sampled signal and then apply corrections. However, the other way around is also possible, with some useful advantages when capturing a more complex signal.

Extracting Signal Components

Extracting the amplitudes and phases from the signal samples crucially depends on the synchronization of the signal source and the sampler. When the source and the sampler operates synchronously and both sampling frequency and number of samples are selected so that exactly an integer number of signal periods are sampled[2], an FFT can be used to extract amplitudes and phases of all signal frequency components without any additional errors attributed to the processing. Whenever such an arrangement is possible, it is arguably the best option to extract spectral components from the sampled data. As the FFT is so well known, we would not discuss it any further here, but for those interested in its proper practical application and the selection and use of windows, a highly recommended freely available source is [5].

Unfortunately, it is not possible to always maintain a coherent sampling. Typically, the reason would be that the source and DMM clocks cannot be synchronized (which is the case for the 3458A), or that the source does not provide a trigger signal (which is the case for today's state-of-the-art multifunction calibrators). In such cases, the DMM sampling clock would run asynchronously to the signal frequency and sampling coherency would not be provided. There are many options for extracting the signal components from asynchronously sampled signal, ranging from interpolated DFT procedures [6], iterative algorithms for a single tone signal estimation [7-8] and iterative algorithms for multi-tone signal estimation [9].

The interpolating DFT procedures are well suited for fast and robust spectral line component estimation, as they use windowed FFT and interpolate the main signal frequency, amplitude and phase from the peak amplitude FFT bin and its adjacent bins amplitude and phase values, without any iteration process. This provides for a very rapid estimation, but the price paid is often an elevated estimated parameter scatter, primarily due to the use of spectral windows. The standard deviation of the estimates can be amplified even a few times above the theoretical lower limit[3], but this performance is predictable and it depends on the actual procedure selected and on the parameter being estimated.

Iterative algorithms are slower but typically still need only a few iterations to reach the final value and processing times below 10 ms, not uncommon with today's computers and a few thousand point record lengths. Well known procedures are three parameter sine fit (3PSF, see Listing 1.) and four parameter sine fit (4PSF) algorithms, which are standardized [7] and fairly popular. The 3PSF is non-iterative but requires a known signal frequency as an input parameter, while the 4PSF is iterative as it solves non-linear problem by also estimating signal frequency. Both 3PSF and 4PSF do not elevate noise over the CRLB, saying that they are noise efficient. However, the 4PSF is fairly sensitive to harmonic distortions present in the sampled signal [10]. To circumvent this shortcoming, a phase sensitive algorithm (PSFE) was developed [8], which significantly reduces the sensitivity to harmonic distortions present in sampled signals to a certain degree, but the price paid is slight (a few percent) and, in practice, is often irrelevant noise elevation. The Matlab script of PSFE procedure is given in Listing 2.

If the PSFE does not provide acceptable performance or one needs to estimate fundamental signal and its harmonics, a multi-frequency sine fit algorithm [9] needs to be applied. Such an algorithm will perform as accurately as FFT when all relevant harmonics are taken into account, but it will require rather large memory and computational time, which will increase linearly with added harmonics.

2 This is often referred to as a coherent sampling.

3 As defined by Cramér–Rao lower bound (CRLB).

Compensating for Known Filter Effects

After the signal parameters (amplitude, phase, in case of asynchronous sampling also frequency) are estimated from the sampled data, they should be compensated for known errors introduced by the DMM. There is no correction to be done for frequency and it is seldom necessary for phase. For amplitude, however, this is achieved by

$$V_{\text{corr}}(f) = \frac{V_{\text{est}}(f)}{H_{t_a}(f) \cdot H_{1p}(f)}, \tag{7}$$

where V_{est} is the estimated amplitude by either FFT or any other algorithm. As both aperture time and input filter behavior have a predictable phase response, they can also be compensated for accordingly [1].

Equalizing Sampled Record for Known Filter Effects Before Extracting Signal Components

The last two steps can also be reversed, in which case the sampled data are first equalized for aperture time and input filter response and the signal components are extracted after that. This can be achieved by applying a digital FIR filter over the input data [1], which would reverse the roll-offs in a maximally flat fashion at low frequencies. For most purposes, a fourth-order FIR filter would provide better than 20 μV/V aperture time roll-off and input bandwidth roll-off equalization up to 3.3 kHz [3] for 3458A at aperture times ≤ 30 μs. Filter coefficients are given exactly by [1]:

$$b_0 = b_4 = \frac{q^2}{288} + \frac{7q^4}{5760} + \frac{\gamma^2}{24} - \frac{\gamma^4}{8}, \tag{8}$$

$$b_1 = b_3 = -\frac{q^2}{18} - \frac{7q^4}{1440} - \frac{2\gamma^2}{3} + \frac{\gamma^4}{2},$$

$$b_2 = 1 + \frac{5q^2}{48} + \frac{7q^4}{960} + \frac{5\gamma^2}{4} - \frac{3\gamma^4}{4},$$

where

$$q = t_a / t_s, \tag{9}$$

$$\gamma = 1/(2\pi f_{3dB} t_s).$$

The filter itself can be implemented by

$$V_{\text{eq}}(n) = \sum_{m=0}^{K} b_m \cdot V(n-m), \tag{10}$$

where K is the FIR filter order (in our case 4).

After such equalization, the actual measured signal components could be extracted from V_{eq} as described before, without any further compensation necessary.

```
function [A, phi, O] = ThreePSF(Record, f, Ts)
 % Three Parameter Sine Fit (3PSF)
 %
 %  [A, phi, O] = ThreePSF(Record, f, Ts)
 %  Input arguments
 %    Record     - sampled input signal
 %    f          - signal frequency
 %    Ts         - sampling time (in s)
 %  Output arguments
 %    A          - estimated signal's amplitude
 %    phi        - estimated signal's phase
 %    O          - estimated signal's offset
 %
 % Reference: IEEE Standard for Digitizing Waveform Recorders
 % IEEE Instrumentation and Measurement Society,
 % IEEE Std 1057TM-2007 (Revision of IEEE 1057-1994)

 N = length(Record);             % determine the number of samples
 Record = Record(:);             % force column vector

 vct = 2*pi*f*Ts*(0:N-1);
 D0 = [cos(vct);sin(vct);ones(1,N)]'; % (Eq. A.3)
 x1 = D0\Record;                 % solve system of linear equations
                                 % (Eq. A.7)
 phi =atan(-x1(2)/x1(1))-pi/2;   % phase estimation (Eq. A.10)
 if x1(1) >= 0                   % wrap phase within <-pi,pi>
   phi = phi + pi;
 end
 A = sqrt(x1(1)^2+x1(2)^2);      % amplitude estimation (Eq. A.9)
 O = x1(3);                      % offset estimation
```

Listing 1. Three parameter sine fit Matlab function

```
function [fa, A, ph, O] = PSFE(Record, Ts)
 % PSFE (Phase Sensitive Frequency Estimator)
 %  [fa, A, ph, O] = PSFE(Record, Ts)
 %
 %  Input arguments
 %    Record     - sampled input signal
 %    Ts         - sampling time (in s)
 %  Output arguments
 %    fa         - estimated signal's frequency
 %    A          - estimated signal's amplitude
 %    ph         - estimated signal's phase
 %    O          - estimated signal's offset
 %
 % PSFE requires more than two periods of sampled signal and
 % at least 6 samples in the Record
 % Reference: Rado Lapuh, "Estimating the fundamental component of
 % harmonically distorted signals from non-coherently sampled data,"
 % IEEE Trans. Instrum. Meas., Vol. 64, No. 6, March 2015, 1419-1424

 N = length(Record);
 Record = reshape(Record,1,N);   % force the row vector
 cost_error = 2.4e-12;           % the cost function threshold error
 max_iter = 20;             % maximum number of algorithm iterations
 NFFT = 2^nextpow2(N);         % Find the initial frequency estimate
 t = fft(Record,NFFT);
 tr = abs(t(1:NFFT/2));
 [~,I]=max(tr);          % find the index of the maximum value bin
 fa = (I-1)/(Ts*NFFT);   % and calculate the corresponding frequency
 if fa == 0              % in case the peak frequency is not found
   A  = NaN; ph = NaN; O  = NaN;
   return
 end
 for iter = 1:max_iter            % the algorithm loop
   dm = fix(N/2);
   if dm < fix(1/(fa*Ts))
     d0 = dm;                     % the optimum window separation d0
   else
     dc = round((round(floor(dm*fa*Ts)/(fa*Ts)):-(1/(fa*Ts)):dm/2));
     dd = dc*fa*Ts;                 % possible candidates for d0
     [~,I] = min(abs(round(dd)./dd-1));
     if I                           % if I is not zero
       d0 = dc(I);
     else
       d0 = dm;
     end
   end
   w0 = N - d0;        % use remaining samples for the window width
   fTs = 2*pi*fa*Ts;
   vct = fTs*(0:w0-1);
   D0 = [cos(vct);sin(vct);ones(1,w0)];
   D0T = D0 * D0';
   D0R = D0 * Record(1:w0)';
   x1 = D0T\D0R;
   ph1=atan(-x1(2)/x1(1));            % W1 phase
   if x1(1) >= 0
     ph1=ph1+pi;
   end
   D0R = D0 * Record(d0+1:d0+w0)';
   x2 = D0T\D0R;
   ph2=atan(-x2(2)/x2(1));            % W2 phase
   if x2(1) >= 0
     ph2=ph2+pi;
   end
   c1 = 2*pi*Ts*d0;
   Dph_a = c1*fa;
   dph_c = ph2 - ph1;
   P = round((Dph_a-dph_c)/(2*pi));  % number of full periods
                                     % between W1 and W2 (Eq. 5)
   Dph_c = dph_c+2*pi*P;             % estimated phase diff. (Eq. 4)
   eps = abs(Dph_a - Dph_c)/c1/fa/N; % cost function result (Eq. 3)
   fa = fa - (Dph_a - Dph_c)/c1;     % new freq. estimate (Eq. 2)
   if eps == 0 || eps < cost_error || iter >= max_iter
     [A,ph,O] = ThreePSF(Record,fa,Ts);
     return
   end
end
```

Listing 2. Phase sensitive frequency estimator Matlab function, which also returns amplitude, phase and offset of a sampled signal.

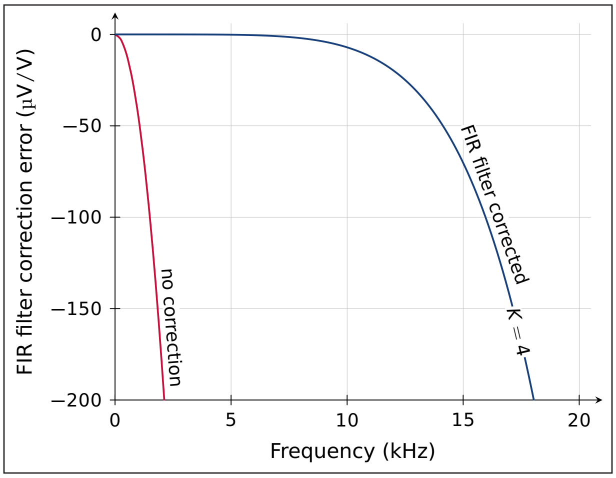

Figure 8. The 3458A's model frequency response error before and after polynomial expansion FIR filter correction.

This approach is very beneficial when dealing with complex signals, as the equalization is performed over all frequencies. The drawbacks are the necessary truncation of the first K+1 samples in the resulting V_{eq}, which represent a convolution with FIR filter settling response and are therefore not accurate and of course not a complete equalization at highest frequencies. The frequency response of the equalization given above is shown on Figure 8.

Conclusion

In this paper, sampling a signal with the popular 3458A type sampling digital multimeter was specifically discussed to measure amplitude and phase of a sinewave signal, but other signal parameters can easily be estimated using the same techniques. By taking the DMM amplitude response model into account, the parameters measured can be estimated with a considerably lower uncertainty. For sampling a complex signal, a digital filter approach was given to equalize sampled raw data for the DMM model response before the signal processing is performed. When the full synchronization between the source and the DMM is not available or practical and the straightforward FTT signal analysis is no longer useful, an asynchronous sine fit algorithm as realized in MATLAB was given to estimate signal parameters. To correctly interpret obtained results, one needs to understand and evaluate actual signal to noise ratio, time jitter and signal distortions, all originating either from the source or from the sampler. With all these techniques applied, it is possible to attain state-of-the-art performance in measurement of a range of low frequency AC parameters, like voltage, phase, low frequency power, power quality parameters and voltage or current ratios.

Bibliography

[1] R. Lapuh, *Sampling with 3458A*, Ljubljana: Left Right d.o.o., 2018.

[2] R. L. Swerlein, "A 10 ppm accurate digital AC measurement algorithm," Agilent Technologies, 1991.

[3] G. B. Gubler, "Reconstruction of bandlimited signal using samples obtained from integration digital voltmeters," CPEM, 2010, pp. 257-258.

[4] R. Lapuh, "Keysight 3458A Frequency Response Model Identification," CPEM, 2018, pp. 1-2.

[5] G. Heinzel, A. Rüdiger and R. Schilling, "Spectrum and spectral density estimation by the Discrete Fourier Transform (DFT), including a comprehensive list of window functions and some new flat-top windows," Max-Planck-Institut für Gravitationphysik, Hannover, 2002.

[6] K. Duda, "Interpolation algorithms of DFT for Parameters Estimation of Sinusoidal and Damped Sinusoidal Signals," Fourier Transformer-Signal Processing, InTech, pp 3-32, 2012. DOI: 10.5772/36264

[7] "IEEE Standard for Digitizing Waveform Recorders," IEEE Std 1057-2007, 2008.

[8] R. Lapuh, "Estimating the Fundamental Component of Harmonically Distorted Signals from Noncoherently Sampled Data," *IEEE Trans, Instrum. Meas.*, 2015.

[9] J. Schoukens, R. Pintelon and G. Vandersteen, "A sinewave fitting procedure for characterising data acquisition channels in the presence of time base distortion and time jitter," *IEEE Trans. Instrum. Meas.*, 1997.

[10] J. P. Deyst, T. M. Sounders and O. Solomon, "Bounds on Least-Squares Four-Parameter Sine-Fit Errors Due to Harmonic Distortion and Noise," *IEEE Trans. Instrum. Meas.*, vol. 44, no. 3, pp. 637-642, 1995.

Rado Lapuh (rado.lapuh@gmail.com), Left Right d.o.o., Ljubljana, Slovenia, www.leftright.eu.

This article is an excerpt taken from Dr. Lapuh's book, *Sampling with 3458A; Understanding, Programming, Sampling and Signal Processing*. The subject of this book is the multimeter model 3458A, first introduced by Hewlett-Packard in 1988. Three decades after its introduction, the 3458A is still unrivaled in some of its characteristics. In electrical measurements, sampling methods are superseding more and more of the traditional analog bridge techniques. This book explains and describes the sampling capabilities of the 3458A multimeter and it gives many examples of its applications. More information may be found at https://leftright.eu/.

Buehler Introduces Wilson® RH2150 Rockwell® Hardness Tester

October 13, 2020, Lake Bluff, IL – Buehler is excited to introduce its newest Rockwell Hardness Tester, the Wilson RH2150, an updated more advanced Rockwell tester with easy programmability, advanced calculations and even verification reminders to ensure compliance. With the launch of the new Wilson RH2150 Buehler celebrates the centennial anniversary of the Wilson brand of hardness testers, test blocks and software.

The RH2150 is available in two different sizes, with a vertical capacity of 10 and 14 inch (254mm and 356mm respectively). It is fully protected from outside influences with sheet metal casing and a load cell protection. Buehler has improved the Rockwell with a terrific clamping device that is attached to the actuator, extended scales, crash protection and a complete new user interface. Early users like the ease of use, great software interface with intuitive icon-based controls, programmability and workflow automation, one button testing and the available accessories, that grant a fully flexible operation for many applications.

According to Matthias Pascher, Hardness Product Manager, "The RH2150 was tested for weeks and months in harsh workshop environments and the consistency of test results and intuitive testing controls is clearly standing out and is the key requirement for this type of hardness testing machine. We designed unique features, such as the clamping device, directly mounted on the actuator, intelligent footswitch controls, or the DiaMet™ software package for advanced testing and reporting solutions, including network connectability which is more and more a need to ensure complete test result traceability."

Furthermore, the machine performs hardness testing according to the current Rockwell standards, as well as plastics and carbon testing scales, and Brinell depth testing scales, all within the load range from 1 to 187.5 kgf. Manufacturing and heat treatment industries that rely on Rockwell can count on this tester being the one that will make their production testing a breeze. With the availability of a large amount of testing scales, this machine also fits perfectly in research labs or testing centers, where operators need to have access to all kinds of scales.

Buehler is a division of Illinois Tool Works (ITW) and is based in Lake Bluff, Illinois. ITW is a global, Fortune 200 company and global industrial manufacturer of value-added consumables and specialty equipment with related service businesses.

Buehler is celebrating the 100-year centennial of the Wilson brand of hardness testers in 2020. For additional information visit www.buehler.com.

New 30,000 lbf Deadweight Load Cell Calibrator added to Morehouse Calibration Laboratory

YORK, Pa., Sept. 21, 2020 (GLOBE NEWSWIRE) -- Morehouse Instrument Company has added a 30,000 lbf automatic deadweight load cell calibrator to its laboratory to dramatically improve force calibration accuracy. The 30,000 lbf machine expands the wide range of calibration equipment at Morehouse, which includes a 120,000 lbf, 12,000 lbf, 1,100 lbf, and 120 lbf deadweight machine.

"Our goal was to achieve more accurate calibrations by designing and building a machine to the highest standards," notes Henry Zumbrun, President of Morehouse. "We accomplished this with a machine that is plumb, level, square, more rigid and has lower torsion than other deadweight machines. Getting all these aspects right is essential to manufacturing a great force standard capable of producing very repeatable results for our customers."

The new 30,000 lbf deadweight machine is 10 to 20 times more accurate than non-deadweight systems. Machines used to calibrate load cells vary from deadweight force standard machines or primary standards with the lowest overall uncertainty to single or multiple transducer machines with higher uncertainty. Some labs even use a universal testing machine or a homemade press to calibrate load cells. Deadweight machines are the most accurate because they are capable of calibrating ISO 376 Class 00, ASTM E74-18 Class AA verified range of forces, AS 2193 Class AA, and other force measuring devices requiring the utmost accuracy. Expanded uncertainty must be better than 50 ppm to assign a Class AA verified range of forces. This is easily achieved with the new 30,000 lbf deadweight machine, which has an expanded uncertainty of 20 ppm.

Morehouse has redesigned many of its automatic deadweight machines with conical lifters so the weights can be lowered by low-pressure air bladders to eliminate shock loading. The redesign also includes more room between weights and a rigid structure. Additionally, the weight complements are designed to eliminate unnecessary hysteresis errors, and weights do not have to be cycled off and on to achieve the necessary force points. The 30,000 lbf deadweight machine includes these design elements to assure the most accurate calibrations.

For more information, contact: Morehouse Instrument Company, 1742 Sixth Avenue, York, PA 17403, (717) 843-0081, Fax (717) 846-4193, www.mhforce.com, info@mhforce.com.

NEW PRODUCTS AND SERVICES

ScalesNet-M Discount

Las Vegas, NV, 10/13/2020 – Effective today, we will be offering the MARO ScalesNet-M Basic Module at a 15% Discount to help Corona Covid19 battered US Mass Metrology Labs to maximize their available investment funding. This 15% Discount is only valid for orders processed within the USA. Please contact 702-763-8828 or email HL-Knobloch@scalesnet-m.com for details or for scheduling a live demonstration.

Robot-supported weight calibration is increasingly finding its way into mass laboratories. This is one reason why ScalesNet-M is subject to permanent development. Every time a new robot, handler or manual balance is introduced by one of the most important balance/comparator manufacturers, it is implemented into ScalesNet-M. This includes the newly introduced Sartorius CCR robot series.

ScalesNet-M is the leading software solution for all tasks in the mass laboratory. From order entry all the way to customer certificate is an easy process: Entering the order number and the serial number of the weight set to be calibrated is enough to activate the record from the archive. After selecting the test object and the reference weight, the calibration can be started. Step-by-step instructions while calibrating weights will guide the user through the process.

After completion of the calibration, all calculated values are immediately displayed on the screen and can be printed and saved. Assessment criteria facilitate a quick statement about the quality of the test sample calibration. All physical effects are recorded and included in the calculations. Freely definable certificates are created at the end of the calibration process.

ScalesNet-M allows communication with all robots, load changers and manual comparators of all relevant manufacturers.

All (multiple) climate stations or data loggers with RS232 or RJ45 interface can be integrated with ScalesNet-M, to be used for automatic data acquisition of the environmental parameters.

For detailed information about ScalesNet-M, visit https://scalesnet-m.com.

Vitrek Announces the SE Series of High Voltage Safety Enclosures

The SE Series offers the utmost in operator safety for high voltage testing with solid aluminum frame construction, a durable acrylic cover and a magnetic interlock safety switch.

Poway, CA, October 13, 2020— Vitrek, a leader in high-voltage test and measurement equipment for over 25 years, introduces its SE Series of high voltage safety enclosures. These products are an important component of providing a safe environment for employees to conduct testing on high voltage devices by preventing electrical shock. Not only does a safety enclosure help to keep the tester safe, but it also protects the device being tested from potential damage. For devices requiring longer test periods, a safety enclosure is recommended as a more reliable means of protection.

Each SE Series product is constructed with a strong, lightweight aluminum frame, with a connection that must be grounded by the customer to ensure safe operation. The acrylic cover is non-conductive, and the enclosure features yellow safety panels and a 20-position terminal block with a removable cover. A 2″ wide flexible grommet allows for cable pass-through, while a large or wide DUT opening makes loading and unloading easier. Each enclosure comes with three high voltage test area stickers to properly notify employees of the potential danger.

Vitrek provides equipment to a wide range of industries, and the company offers three different models that fit many common devices. Customers can choose an optional insulation mat to complement the safety enclosure. Their experienced engineering team can also create customized units to fit specific applications.

"In high voltage testing, the safety of operators is paramount," said Chad Clark, Vitrek's VP Sales & Marketing. "Vitrek is proud to be able to offer the SE Series of safety enclosures to assist companies in creating a safe working environment."

Every product included in Vitrek's Electrical Safety and Test Equipment Catalog is American-made in San Diego, California and comes with the same outstanding level of customer support, features and performance quality Vitrek customers have relied on for over 25 years.

View online: https://vitrek.com/se-series-safety-enclosures/

The Ralston Quick-test Connection Platform

The Ralston Quick-test Connection Platform is a universal pressure hose system engineered to facilitate fast, leak-free connections for pressure testing, calibration, and leak testing. The unique design of our hoses and adapters offers secure, time-saving connections - without the need for a wrench or thread tape - for low volume, high pressure connections to virtually any device being tested.

Ralston Quick-test hoses are an industry first. They have a smaller inner diameter than most hoses, which makes them ideal for transmitting high pressure without wasting large amounts of compressed gas or fluid. And because they're made with a polyamide-reinforced inner core, they can twist and bend without losing volume across the hose. Ralston Quick-test Adapters are a perfect complement to the hoses. They allow direct connection to male or female NPT, BSPP, Tube Fittings, Metric, AN 37° Flare and CGA 580 fillings without any additional tools or thread sealant. They can also vent pressure while still connected, and because they eliminate the need for wrenching, the threads don't wear out.

The Ralston Quick-test Connection Platform was designed for simplicity and ease of use. For more information, contact Ralston Instruments at ralstoninst.com/cm-qt or call 800-347-6575 for more information.

International Digital Calibration Certificate

Michael L. Schwartz
Cal Lab Solutions, Inc.

In the past 20 years, having a digital representation of a calibration certificate has been a topic of discussion. I remember attending my very first NCSLI Workshop & Symposium in 2001 and sitting in on the 141 Automation Committee meeting discussing this very topic. The only thing we could agree on back then was the file format should be XML. But unfortunately, the only thing we have been able to accomplish since then is more calibration labs offer a PDF version of a calibration certificate and call that a digital format.

Well, it would seem the world has come full circle and we are again working to create a standard for digital calibration certifications. Only now there is a worldwide effort of people, companies, and National Metrology Institutes (NMIs) all working on the problem of Digital Calibration Certificates—each with an XML definition, hoping other organizations will adapt their standard.

This was my comment at my first ever NCSLI 141 committee meeting: "Yes, XML is a great technology but who is going to define the XML Schema?" 19 years later we are still asking the same question. But the encouraging news is now there are several published schema that we can evaluate and possibly implement.

The schema, or as it is known XSD file, is a formal definition of how the XML file and its elements are formatted. See, XML files in a sense are mini-database organized in a hierarchical format from the root node to all of its elements. The specified name of each element, parent-child relationships, and attributes are formally defined in the XSD Schema File, thus making it the key or map to all the data in the file.

This week, PTB (Physikalisch-Technische Bundesanstalt), Germany's NMI, held a virtual conference called the DCC 2020 workshop covering information, adoption, and presentation about digital calibration certificates. Over the past year, there have been a lot of tools and middleware applications built around their XML Schema. If you would like to learn more just visit https://www.ptb.de/dcc.

PTB's DCC is a great format from the NMI Level, focused on measurement and uncertainty values. But the production calibration labs at the bottom of the metrology pyramid are more interested in Pass/Fail limits with tolerances. They want to know what is their risk, and can they use the instrument to make measurements or not. This was discussed in this year's DCC virtual conference and may get added in the future. Also, the topic of accredited vs. non-accredited calibration data was addressed. I didn't know this, but they mentioned some NMIs are not accredited like most calibration laboratories.

Another great paper from Miguel Margus, with INEGI (Institute of Science and Innovation in Mechanical and Industrial Engineering) of Portugal, presents a great schema layout but it brings up an interesting problem: What language should the schema be writing in, what date and time format, and what number format? There are a lot of things that need to be definitely addressed in the schema, such as Americans like the Month/Day/Year format, while Europeans like the Day/Month/Year format. NATO addressed this problem with the 01-Jan-20 format that is non-ambiguous, as well as the worldwide adoption of Zulu Time or UTC (Coordinated Universal Time).

Earlier this year, at NCSLI's 2020 virtual conference, Collin Delker with Sandia National Labs presented a paper "Exploration of a Data-Enhanced Calibration Certificate as Part of a Complete Measurement Information Infrastructure." This paper was quite interesting in that it doesn't solve the international language or formation problems, but provides the best of both worlds by combining XML and PDF in one file. Instead of representing everything in an XML format, the XML data is embedded into the PDF. You can download and read this paper from NCSLI's 2020 Conference proceedings at https://www.ncsli.org.

Whether it is embedded in the PDF or a standalone XML file, we have a lot of ground to cover as we work to create an International Digital Calibration Certificate schema representation of the calibration data that is transportable from system to system. I think we all need to look at all of the proposed standards, compare and contrast them, and look at what expansion we need to make to our data formats. We also need to think about how we can provide feedback on what is missing from each format that is out there. ❧

Additel

Metrology Made Simple

Additel 875-1210 and 878-1210 Thermocouple Calibration Furnaces

- *Temperature control from 100°C to 1210°C*
- *Two models to choose from: Reference (ADT878) and Standard (ADT875)*
- *Display Accuracy of ±1.5°C (ADT878)*
- *4 on-board measurement channels (PC option)*
- *Portable, rugged and quick to temperature*
- *Self-calibration feature (PC option)*
- *Portable, designed for use in the field and in the lab*
- *ISO 17025-accredited calibration w/data included*
- *Multi-zone temperature control*
- *Internal and external sensor control (PC option)*
- *Metallic interchangeable inserts*
- *Wi-Fi and Bluetooth capable*
- *Color touch screen display*

Phone: 714-998-6899
Fax: 714-998-6999
E-mail: sales@additel.com

Corporate Headquarters
2900 Saturn Street #B
Brea, CA 92821, USA

Salt Lake City Office
1364 West State Rd. Suite 101
Pleasant Grove, UT 84062, USA

www.additel.com